International Journal of Nanomedicine Dovepress

Open Access Full Text Article ORIGINAL RESEARCH

Simulated Gastrointestinal Fluids Impact the Stability of Polymer-Functionalized Selenium Nanoparticles: Physicochemical Aspects

Atiđa Selmani[1], Nives Matijaković Mlinarić[2], Salvatore Fabio Falsone[1], Ivan Vidaković[3], Gerd Leitinger[4], Ida Delač[5], Borna Radatović[5], Ivan Nemet[6], Sanda Rončević[6], Andreas Bernkop-Schnürch[7], Tomislav Vuletić[5], Karin Kornmueller[3], Eva Roblegg[1], Ruth Prassl[3]

[1]Department of Pharmaceutical Technology and Biopharmacy, Institute of Pharmaceutical Sciences, University of Graz, Graz, 8010, Austria; [2]Laboratory for Precipitation Processes, Division of Material Chemistry, Institute Ruđer Bošković, Zagreb, Croatia; [3]Division of Medical Physics and Biophysics, Gottfried Schatz Research Center for Cell Signaling, Metabolism and Aging, Medical University of Graz, Graz, 8010, Austria; [4]Division of Cell Biology, Histology and Embryology, Gottfried Schatz Research Center for Cell Signaling, Metabolism and Aging, Medical University of Graz, Graz, 8010, Austria; [5]Center for Advanced Laser Techniques, Institute of Physics, Zagreb, 10000, Croatia; [6]Department of Chemistry, Faculty of Science, University of Zagreb, Zagreb, 10000, Croatia; [7]Center for Chemistry and Biomedicine, Department of Pharmaceutical Technology, Institute of Pharmacy, University of Innsbruck, Innsbruck, 6020, Austria

Correspondence: Ruth Prassl, Medical University of Graz, Neue Stiftingtalstraße 6, MC2.H.3.31, Graz, 8010, Austria, Tel +43 (0) 316 385-71695, Email ruth.prassl@medunigraz.at

Background: Selenium (Se) is a vital micronutrient for maintaining homeostasis in the human body. Selenium nanoparticles (SeNPs) have demonstrated improved bioavailability compared to both inorganic and organic forms of Se. Therefore, supplementing with elemental Se in its nano-form is highly promising for biomedical applications related to Se deficiency.

Purpose: The primary objective of this study was to evaluate the impact of the main gastrointestinal proteins on the physicochemical properties and stability of polymer-coated SeNPs.

Methods: SeNPs functionalized with thiolated chitosan or hyaluronic acid were characterized based on their composition, morphology, size, and zeta potential. The stability of these particles was evaluated in simulated gastric and intestinal fluids. Additionally, the interaction propensity between major gastric proteins, such as pepsin and pancreatin, and functionalized SeNPs was investigated with FTIR, fluorescence quenching titrations, and in situ adsorption measurements.

Results: The composition of the media, including pH and ionic strength, the chemistry of polymers, and the presence of the proteins, influence the size and zeta potential of the SeNPs. The increase in NP size due to the formation of large agglomerates, along with the decrease in zeta potential magnitude, confirmed the formation of a protein corona. Both pepsin and pancreatin showed a strong affinity to the particle surface. Based on the values of the apparent equilibrium dissociation constant this affinity was more pronounced for positively charged thiolated chitosan coated SeNPs compared to those coated with negatively charged hyaluronic acid. The polymer coated SeNPs displayed antioxidative potential, which could be very beneficial for health conditions associated with Se-deficiency.

Conclusion: This study highlights the importance of exploring the characteristics of polymer-functionalized SeNPs under gastrointestinal conditions. Such investigations are important for developing nutritional supplements that can gradually release Se from SeNPs, thereby improving selenium absorption, bioavailability, and safety.

Keywords: nanoparticles, thiolated chitosan, hyaluronic acid, gastrointestinal proteins, bio-nano interface, protein corona

Introduction

Selenium (Se) is an essential trace element incorporated into selenoproteins, which regulate physiological processes such as the modulation of inflammatory responses, cell signaling, and various metabolic processes in the human body.[1] Adequate Se intake in the everyday diet is crucial for maintaining body homeostasis and preventing health problems associated with poor Se intake or low Se absorption.[2] Plants are the primary source of Se, which then enters the food chain, however, the distribution of Se in soil is not globally uniform. Due to this uneven distribution of Se, the daily

Received: 18 June 2024
Accepted: 10 November 2024
Published: 17 December 2024

Graphical Abstract

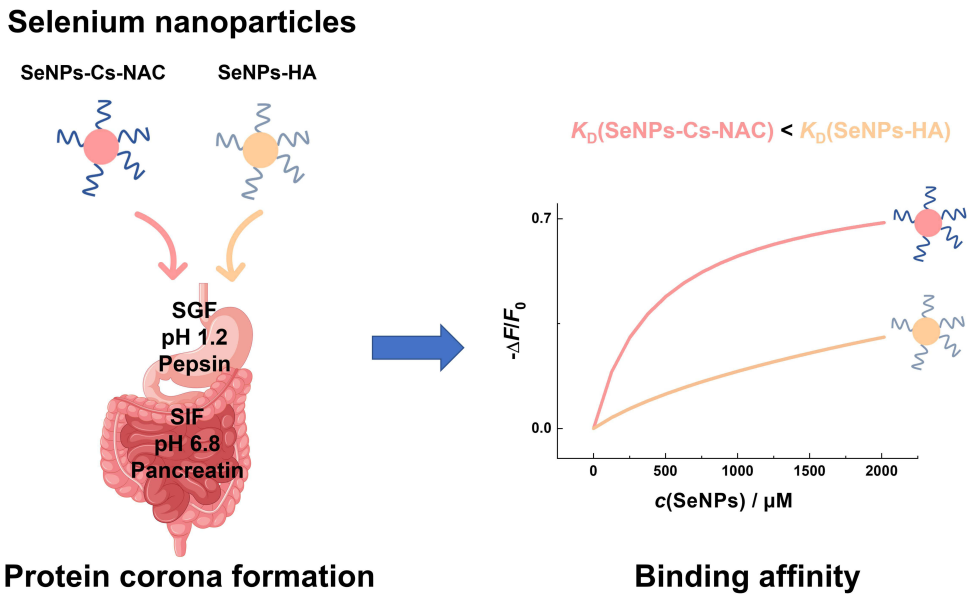

uptake of Se may be compromised and might need to be enriched by nutritional supplementation.[3] Currently, Se supplementation primarily relies on inorganic and organic Se compounds, which have a narrow therapeutic window between toxic and beneficial effects. As an alternative to classical Se compounds, Se in its nano-form synthesized as Se nanoparticles (SeNPs) has attracted interest due to its lower toxicity, biodegradability as well as anti-oxidative, anti-microbial, anti-inflammatory, and anti-tumor properties.[4] Accordingly, SeNPs with varying compositions, crystallinity, size, morphology, and surface charge that are critical quality attributes, have been synthesized and optimized to improve the bio-efficacy and pharmacokinetic profile of Se.[5–10]

Oral drug administration is one of the most exploited and preferred administration routes to improve patient compliance. However, drugs have to pass the harsh conditions in the gastrointestinal (GI) microenvironment. In the GI-tract (GIT), drug degradation and inactivation may lead to insufficient bioavailability of the drug, frequently hindering its effectiveness as a therapeutic agent.[11] Recent studies have shown that SeNPs exhibit minimal side effects and toxicity under GI-conditions. This is attributed to the limited release of Se ions, regardless of the varying pH values in the GIT.[12,13] However, the size and stability of SeNPs may undergo alterations upon entering the GIT due to different enzymatic and pH conditions. It is well known that NPs have the propensity to adsorb a layer of proteins, polysaccharides, lipids, and nucleic acids forming the so-called "protein corona" (PC) at a bio-nano interface.[14] More specifically, a bio-nano interface can be formed between the surface of NPs and biological molecules via electrostatic, van der Waals, covalent, steric, or hydrophobic interactions.[15,16] This means that the PC formation could interfere with NP's stability, cell internalization, biodistribution, and immune response. To date, most published research is oriented on PC formation in the blood[17–21] although some recent studies specifically focus on PC formation in simulated gastric (SGF) or intestine fluids (SIF).[22–26] In general, NPs intended for oral application must be optimized not only to prevent degradation but also to enhance biodistribution and penetration through GI-barriers. Specifically, the binding of enzymatic proteins to the surface of NPs increases their size and modifies their surface properties. This, in turn, affects their interaction with and infiltration through the mucus layer, impacting the uptake mechanism and cellular entry.[27] Therefore, understanding the fate of the NPs upon encountering GIT is important.

To improve the stability and biological behavior of NPs, they are frequently coated and functionalized by polymers that show excellent biocompatibility, low toxicity, in vivo biodegradability, and the ability to bind to the mucus layer or to pass across mucosal barriers.[28] When NPs are coated with polysaccharides such as chitosan (Cs) or hyaluronic acid

(HA), they can also exhibit immunomodulatory effects by decreasing the production of inflammatory cytokines and regulation of CD44 and TLR4 receptor expression.[29,30] HA, which is found in the extracellular matrix of the gastrointestinal mucosa serves as a barrier to protect the epithelium. Moreover, HA plays an essential role in healthy intestinal tissue homeostasis, and high molecular weight HA was shown to exhibit significant anti-inflammatory effects.[31] Based on such beneficial properties, Cs and HA were recognized as polymers with enormous potential in the biopharmaceutical and biomedical fields. As functional pH-responsive polymers Cs and HA have a protective role in the GIT enabling a controlled release of NPs. For example, in the work of Gue et al, the fate of CsNPs was evaluated in a 3-phase GIT simulator.[32] It was shown that CsNPs do not dissolve in the gastric fluid, while a small aggregation of NPs was detected in the intestinal fluid. However, the polymers are susceptible to the intrinsic features of GIT (pH, salts, enzymes) that could alter their integrity in terms of surface charge and structure, thus leading to limited stability and an impaired release profile of NPs, potentially reducing their therapeutic effectiveness.[33]

Accordingly, derivatization of polymers might be a promising strategy to improve their physicochemical properties, release profiles, adhesion to biological barriers, and internalization within cells.[34,35] One such example is thiolated polymers, designated thiomers.[36] Thiomers commonly consist of free thiol group-bearing agents immobilized to a polymeric backbone. The immobilized thiomers (free SH-groups) interact with the cysteine-rich subdomains on the protein surface in the mucus layer of GIT, thus forming disulfide bonds.[12,37] To take advantage of this feature, thiolated Cs (Cs-NAC) was used in this study instead of plain Cs, in similar way as published previously.[12,38] Regarding nutritional supplements, a synergism between the beneficial properties of functional polymers and SeNP is expected to improve the bio-efficacy of SeNPs as well as their anti-oxidative potential, which is an essential characteristic of the potential nutritive supplement.

In this study, we aimed to investigate the behavior of Cs-NAC and HA-functionalized SeNPs under GI conditions and to address the interaction with major GI proteins, particularly pepsin and pancreatin. We intended to examine the affinity of these proteins for SeNPs in dependence on the type of the coating agent, pH, and ionic strength of the media (simulated gastric fluids). For this purpose, polymer-coated SeNPs were fabricated by a facile chemical reduction synthesis, followed by the determination of their physicochemical characteristics (composition, morphology, size distribution, and surface charge). The interactions between polymer-coated SeNPs and proteins were probed by Fourier transform infrared (FTIR), quartz crystal microbalance with dissipation monitoring (QCM-D), and fluorescence titration spectroscopy. We found that gastric proteins bind to the particle surface leading to PC formation. The binding affinity strongly depended on the type of polymer coating used. The data obtained could aid in building up a design platform for SeNPs as a nutritional supplement, which opens up new prospects for an efficient and gradual release of Se after ingestion, particularly in the mitigation of health conditions associated with Se deficiency.

Materials and Methods

Materials

Sodium selenite (Na_2SeO_3) was purchased from Thermo Fisher GmbH (Kandel, Germany), and L(+)-ascorbic acid and hydrochloric acid (HCl, w = 36%) were purchased from Carl Roth GmbH & Co (Karlsruhe, Germany). Chitosan-N-acetyl-cysteine (Cs-NAC, $M_w \approx 150$ kDa) was synthesized and supplied by Thiomatrix® (Innsbruck, Austria).[38] Hyaluronic acid sodium salt (HA) from *Streptococcus equi* ($M_w \approx 1500 - 1800$ kDa), pepsin from porcine gastric mucosa, pancreatin (mixture of the trypsin, amylase, lipase, ribonuclease, and protease) from porcine pancreas, mannitol, sodium bicarbonate ($NaHCO_3$), 2-mercaptoethanol, sodium dodecyl sulphate (SDS) and 2,2-diphenyl-1-picrylhydrazyl (DPPH) were purchased from Sigma® Aldrich (Vienna, Austria). Ellman's reagent (5,5- dithiobis-2-nitrobenzoic acid, DTNB) was purchased from Thermo Fischer (Vienna, Austria). A phosphate buffer (PBS, pH = 7.4) was prepared by mixing sodium dihydrogen phosphate monohydrate and disodium hydrogen phosphate dihydrate, which were also provided by Carl Roth (Karlsruhe, Germany). All solutions were prepared with ultra-pure water, Milli-Q water (MQ-water, resistivity of 18.2 MΩ cm^{-1}, Academic water purification system, Millipore GmbH, Vienna, Austria).

Methods

Preparation of Selenium Nanoparticles (SeNPs)

SeNPs were synthesized as described previously with slight modifications.[12] Briefly, 4 mL of aqueous solution of 0.1 M Na_2SeO_3 was mixed with 1 mL of 10 mg/mL of Cs-NAC (Figure 1a) or 1 mL of 1 mg/mL of HA (Figure 1b) under magnetic stirring for 10 min. Next, 10 mL of a 0.1 M aqueous solution of ascorbic acid was added. The reaction was stirred for 10 min at room temperature. The change in the color of the solution from colorless to orange or red was an indicator of the chemical reduction of selenium and the formation of SeNPs-Cs-NAC/-HA, respectively. After the synthesis, the samples were dialyzed in a dialysis membrane (Carl Roth GmbH & Co, Karlsruhe, Germany) with a 14 kDa cut-off in MQ-water for 24 h. During the dialysis, the media was changed three times. The purified SeNP suspensions were freeze-dried with VirTis BenchTop Freeze Dryer 3L (company, Country) using mannitol as a cryoprotectant for 48 h. Briefly, 8 mL of SeNP suspension was mixed with 0.08 g of mannitol to obtain SeNP suspensions with 1% w/v mannitol in vials for lyophilization.[39] The vials were sealed with parafilm and put in the freezer at −80 °C overnight, followed by lyophilization. The lyophilized samples were stored in a climate chamber (ICH110, Memmert GmbH + Co. KG, Schwabach, Germany) at 25 °C for 12 months. During that period the samples preserved their integrity as confirmed by visual inspection. Before use, the samples were reconstituted by suspending them in 8 mL of MQ-water. The lyophilized and rehydrated SeNPs-Cs-NAC/-HA were used for further experiments.

Quantification of Free Thiol Groups Using Ellman's Assay

The amount of free thiol groups of Cs-NAC was determined with the Ellman's assay. Briefly, Ellman's reagent, DTNB was dissolved in MQ-water at the final concentration of 7.5 mm. An aqueous solution of 1 M $NaHCO_3$ was slowly added until pH = 8 was reached that enabled the complete dissolution of DTNB. 2-mercaptoethanol in a concentration range from 25 µM to 5 mm was used as the standard reagent. The Ellman's assay was performed on a 96-well-plate (Cellstar®, Greiner Bio-One, Kremsmünster, Austria). 10 µL of Cs-NAC and standard solutions were mixed with 150 µL of PBS buffer, followed by the addition of an aqueous solution of 40 µL of DTNB. The samples were incubated for 30 min in the dark and the absorbance was recorded at 412 nm with a Clariostar® plate reader (BMG LABTECH GmbH, Ortenberg, Germany).

Preparation of Simulated Gastric Fluid (SGF) and Simulated Intestinal Fluid (SIF)

SGF_0 (without enzyme), SGF (with pepsin), SIF_0 (without enzyme), and SIF (with pancreatin) were prepared according to the US Pharmacopeia (26th Edition, 2003). Briefly, SGF was prepared by mixing 2 g of sodium chloride, 3.2 g of pepsin, and 7 mL of hydrochloric acid per L (w = 36%); pH 1.2. SIF was prepared by mixing 6.8 g of potassium phosphate, 10 g pancreatin, and 77 mL of 0.2 M sodium hydroxide per L; pH 6.8. SGF_0 and SIF_0 were prepared in the same manner without adding enzymes.

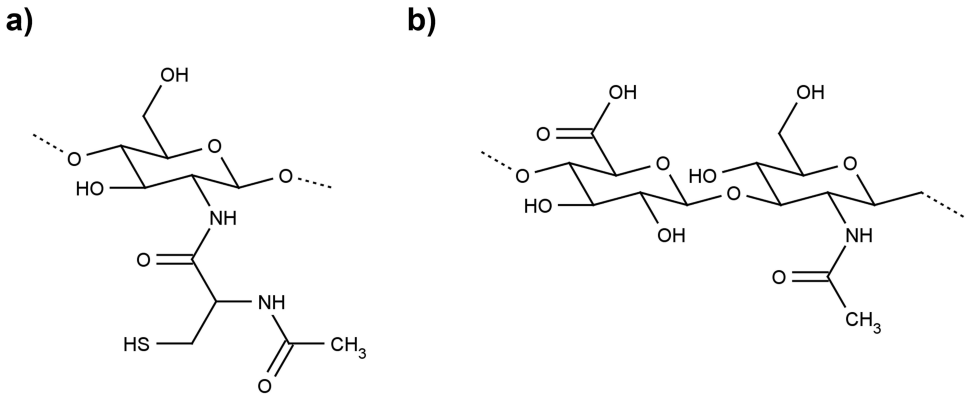

Figure 1 Schematic diagram of the substructure of (**a**) chitosan-*N*-acetyl cysteine (Cs-NAC) and (**b**) hyaluronic acid (HA).

Physicochemical Characterization of SeNPs

Composition and Crystallinity of SeNPs

The composition and crystallinity of coated SeNPs were determined with powder X-ray diffraction (PXRD measurements). PXRD patterns were recorded by an Aeris Benchtop X-Ray diffractometer (Malvern Panalytical Ltd., Malvern, United Kingdom) with Ni-filtered copper radiation in Bragg-Brentano geometry. The samples were deposited on silicon zero-background holders, and patterns were recorded in the range 2θ = 5–70 ° with a step size of 0.005 ° and 10s per step. The PANalytical High Score Plus 4.5 software suite (Malvern Panalytical Ltd., Malvern, United Kingdom) was used for data evaluation.

Morphology of SeNPs

The morphology of the lyophilized SeNPs-Cs-NAC/-HA samples was investigated by scanning electron microscopy (SEM) using a Tescan Vega3 LMU (Brno, Czech Republic) with tungsten filament at 6- and 12-mm working distance, 5–30 kV acceleration voltage. Small amounts of SeNPs, either coated with Cs-NAC or HA were placed on a sample holder with carbon tape. The excess powder was removed by nitrogen gas flow. The morphology of the SeNPs-Cs-NAC/-HA after rehydration was examined by transmission electron microscopy (TEM). TEM imaging was performed with a Fei Tecnai G^2 20 transmission electron microscope (Eindhoven, The Netherlands) operating at 120 kV acceleration voltage. Digital images were recorded using a Gatan US1000 CCD camera at 2K x 2K resolution and the Digital Micrograph software (Version 1.93.1362, Gatan Inc., Pleasanton, USA). The lyophilized SeNPs-Cs-NAC/-HA were dispersed in MQ-water, and 10 µL of the sample was placed on a carbon-coated copper grid, left for 1 minute, and blotted away with filter paper. Negative staining was done with 1% (w/w) uranyl acetate solution twice for 1 minute each. Finally, the samples were allowed to air dry for TEM visualization. Sizes of SeNPs from SEM and TEM images were obtained by using ImageJ software (Version 1.53p) and analysis of 50 particles from SEM and 30 particles from TEM images.

Size and Zeta Potential of SeNPs

Mean particle diameters of SeNPs-Cs-NAC/-HA after dialysis, lyophilization, and rehydration were determined by dynamic light scattering (DLS) using the Litesizer 500 (Anton Paar, Graz, Austria). The device was equipped with a semiconductor laser diode (40 mW) operating at 658 nm. The measurements were performed at an angle of 90 ° (side scattering). 100 µL of 100 mg/L of SeNPs was mixed with 900 µL of MQ-water. Measurements were conducted at 25 °C. The data were evaluated with Kalliope Version 1.2.0 software (Anton Paar, Graz, Austria). The particle size distribution and zeta potential of SeNPs-Cs-NAC/-HA after lyophilization, rehydration, and incubation with SGF_0 /SGF and SIF_0/SIF were determined with the Zetasizer Nano ZS (Malvern Panalytical, Worcestershire, UK). For the DLS and electrophoretic light scattering (ELS) measurements, a He/Ne red-light-emitting laser (λ = 633 nm) was used. The particle size was determined at an angle of 173 ° (backscatter mode). 250 µL of 2 mg/mL of SeNPs-Cs-NAC/-HA was mixed with 750 µL MQ-water and vortexed before the measurements, which were conducted at 25 °C. The data were processed with Zetasizer software 6.32 (Malvern Panalytical, Worcestershire, UK). The zeta potential of the SeNPs was calculated from the measured electrophoretic mobility by applying the Henry equation using the Smoluchowski approximation (f(κa) = 1.5).

Protein Corona Formation

Protein corona formation was studied as described by Wang et al, with slight modifications.[24] Briefly, 0.5 mL of 1 g/L SeNPs-Cs-NAC and SeNPs-HA were mixed with 1.5 mL of SGF_0/SGF or SIF_0/SIF. Samples were incubated in SGF_0 /SGF for 30 min and in SIF_0/SIF for 2 h at 37 °C in a thermo shaker (Thermomixer comfort, Eppendorf Austria GmbH, Vienna, Austria), shaken at 100 rpm, followed by centrifugation (Centrifuge 5804 R, Eppendorf Austria GmbH, Vienna, Austria) at 20817 g for 20 min. The precipitate was washed 3 times with MQ-water to remove unbound proteins, followed by dispersing in MQ-water and subjected to size and zeta potential measurements as described in the previous section. As a control, the zeta potential of pepsin and pancreatin in SGF and SIF was measured, respectively. For the Fourier transform infrared spectroscopy (FTIR) measurements, the SeNPs-Cs-NAC/-HA were incubated with gastric

fluids as described above, followed by a washing step with MQ-water, centrifugation (at 20817 g for 20 min), and lyophilization (described in the section Preparation of selenium nanoparticles (SeNPs) before measurements. The FTIR spectra were recorded with a PerkinElmer FTIR C89391 device (Perkin Elmer, Waltham, USA) at room temperature, in the spectral range of 4000 to 400 cm^{-1}, with a resolution of 2 cm^{-1}.

Determination of the Binding Affinity of Gastric Proteins for SeNPs

In-Situ Adsorption

For the in-situ monitoring of the interactions of pepsin or pancreatin with SeNPs-Cs-NAC/-HA quartz crystal microbalance with dissipation monitoring (QCM-D) was employed utilizing a Q-Sense E1 instrument (Biolin Scientific AB, Gothenburg, Sweden) and as sensors the gold-coated AT-cut quartz crystal (QSX-301, Biolin Scientific AB, Gothenburg, Sweden) with a fundamental frequency of 4.96 MHz. Parameters of resonant frequency, Δf and ΔD dissipation were recorded for several odd overtones, however, for the analysis the 3rd harmonic parameters' values were used. The Au sensor was cleaned every time before the measurement, following the manufacturer's recommendations: immersion into 2% SDS for 30 min followed by thorough rinsing with ultrapure water and drying with nitrogen gas. Dried sensors were treated with O_2 plasma for 10 minutes in Diener Zepto plasma oven (Ebhausen, Germany). The adsorption procedure was as follows. MQ-water was introduced in the flow cell until a stable baseline of the frequency (Δf) and dissipation energy (ΔD) was detected, and then SGF or SIF was injected and the adsorption of gastric enzymes on the Au surface was followed. Loosely bound gastric proteins were washed away with enzyme-free SGF_0 or SIF_0. SeNPs-Cs-NAC/-HA (250 mg/L) were suspended in enzyme-free SGF_0 or SIF_0 and injected into the flow cell, followed by a washing step to remove the unbound SeNPs. All experiments were performed at 37 °C with a flow rate of 100 µL/min.

Fluorescence Quenching Titration Experiments

To quantify the binding affinity of SeNPs-Cs-NAC and SeNPs-HA to pepsin or pancreatin, fluorescence quenching titrations were performed, taking advantage of the intrinsic tryptophan fluorescence of these proteins. Measurements were done using a Jasco FP-6500 spectrofluorometer (Jasco, Tokyo, Japan) at 25 °C. Emission spectra were recorded between 300 and 400 nm upon excitation at 295 nm. Fluorescence signal variations of a 20 µM pepsin solution, corresponding to a physiological concentration of 0.8 mg/mL, were recorded upon the stepwise addition of SeNPs-Cs-NAC/-HA. In the case of pancreatin, a 0.2 mg/mL pancreatin solution was applied.

To derive the dissociation constants (K_D) for the binding of pepsin/pancreatin to SeNPs-Cs-NAC/-HA, the normalized fluorescence intensity changes $-\Delta F/F_0$ resulting from three independent background-corrected experiments were plotted as a function of increasing SeNPs-Cs-NAC/-HA concentration. The curves were fitted by non-linear regression according to equation 1:

$$F = F_0 + F_{max}\frac{K_D + [\text{protein}] + [\text{NPs}] - \sqrt{(K_D + [\text{protein}] + \left[\text{NPs}\right]^2) - 4[\text{protein}][\text{NPs}]}}{2[\text{protein}]} \quad (1)$$

where F is the observed fluorescence signal change $-\Delta F/F_0$, F_0 is the initial fluorescence intensity (set to zero for normalized curves); F_{max} is the maximal fluorescence intensity at binding saturation; K_D is the dissociation constant; [protein] is the concentration of pepsin; [NPs] is the concentration of SeNPs-Cs-NAC/-HA.[40] Due to the heterogeneous composition of pancreatin, a quantitative derivation of the K_D values was precluded. To obtain apparent K_D values for relative comparison, a deliberate concentration of 10 µM pancreatin was assumed for fitting to equation 1.

DPPH Assay

To test the radical scavenging potential of the SeNPs-Cs-NAC/-HA, a DPPH assay was performed using the stable free radical DPPH.[12] Briefly, 100 µL of SeNPs-Cs-NAC/-HA in PBS buffer (pH = 7.4) were mixed with 100 µL of 0.4 mm ethanolic DPPH solution. The final concentrations of the SeNPs-Cs-NAC/-HA were 10, 25, 50, 75, and 100 mg/L. Samples were incubated for 30 min in the dark at room temperature. As the blank probe, DPPH mixed with ethanol was used, while as the positive control, 1 and 10 mm ascorbic acid in PBS buffer were used. The absorbance was measured at

517 nm using the Clariostar® plate reader (BMG LABTECH GmbH, Ortenberg, Germany). The free radical scavenging potential (FRS / %) was calculated from equation 2:

$$\mathrm{FRS}/\ \% = \left(\frac{A_0 - A_{\mathrm{sample}} + A_{\mathrm{blank}}}{A_0}\right) 100 \quad (2)$$

where A_0 is the absorbance value of the free radical DPPH without NPs, A_{sample} is the absorbance of the DPPH radical after incubation with NPs, and A_{blank} is the absorbance value of NPs at 517 nm.

Statistical Analysis

The measured values are expressed as means ± standard deviation (SD). The number of repetitions performed for each experiment is indicated. The differences between groups were analyzed by an unpaired Student's *t*-test using the program GraphPad Prism 8 (La Jolla, CA, USA). Statistical significance was assigned as * $p < 0.05$, ** $p < 0.01$, *** $p < 0.001$, **** $p < 0.0001$ where a p-value <0.05 was considered statistically significant.

Results

Quantification of Free Thiol Groups Using Ellman's Assay

The amounts of free thiol groups in Cs-NAC after coupling with Cs was determined by the Ellman's assay revealing 268 µmol per g of polymer. Based on this, it can be calculated that 4.3% of all amino-groups in Cs are thiolated via NAC. Consequently, the estimated ratio of the primary amines to thiols is 95.7: 4.3.

Synthesis and Characterization of SeNPs

This study employed a facile and highly efficient chemical reduction synthesis to obtain SeNPs coated with Cs-NAC or HA. More precisely, SeNPs were fabricated by mixing Na_2SeO_3 with Cs-NAC or HA. After a short time of incubation, ascorbic acid was added to result in SeNP formation, confirmed by the change in color of the reaction mixture from transparent to orange (SeNPs-Cs-NAC) or red (SeNPs-HA). The chemical reaction that resulted in SeNPs-Cs-NAC/-HA formation is presented by equation 3:

$$SeO_3^{2-} + 2C_6H_8O_6 + 2H^+ \rightarrow Se + 2C_6H_6O_6 + 3H_2O \quad (3)$$

The presence of Cs-NAC and HA facilitates the stabilization of SeNPs during their formation, while bare SeNPs are highly unstable with a strong tendency to aggregate and precipitate in aqueous solution.[5,41] Importantly, the synthesis procedure for SeNPs is fast and straightforward and the use of biocompatible and biodegradable water-soluble polymers yields functionalized SeNPs within a few minutes. After synthesis and dialysis in MQ-water, the samples were lyophilized to provide long-term stability of SeNPs-Cs-NAC/-HA to be applied as a possible nutritional supplement. Mannitol was added in a small amount to protect the SeNPs during the lyophilization process and to facilitate their reconstitution after the lyophilization process.[39]

The composition and crystalline/amorphous structure of SeNPs-Cs-NAC/-HA were determined by PXRD (Figure 2a). SeNPs-Cs-NAC exhibited a broad diffraction pattern at 2θ / °= 25.3 corresponding to the (100) plane, while for SeNPs-HA, two broad reflections were observed at 2θ / °= 28.1 and 40.9, corresponding to the (101) and (110) planes, respectively. The broad reflections observed in the PXRD diffractogram indicated the amorphous structure of the SeNPs. This is in line with our earlier study, where the SeNPs were encapsulated in Cs-NAC coated liposomes.[12] Interestingly, in the work published by Bai et al, the SeNPs were prepared by the addition of unmodified Cs, and the authors visualized broad reflections, as well as sharp peaks in the diffractogram.[42] This finding is characteristic of the variability of SeNPs to adopt both amorphous and crystalline structures depending on the polymer and the manufacturing conditions. Along this line, the effect of the different coating agents on the structure of SeNPs was observed in a study by Selmani et al, where surface agents such as the polymers polyvinylpyrrolidone, poly-L-lysine, polyacrylic acid resulted in amorphous SeNPs.[43] Conversely, when the surfactant sodium bis(2-ethylhexyl) sulfosuccinate was used as a coating agent, the SeNPs exhibited a crystalline structure that corresponded to trigonal Se. Surfactants are often used as morphology-directing agents,[44] while polymers are often used to inhibit crystallization from supersaturated solutions

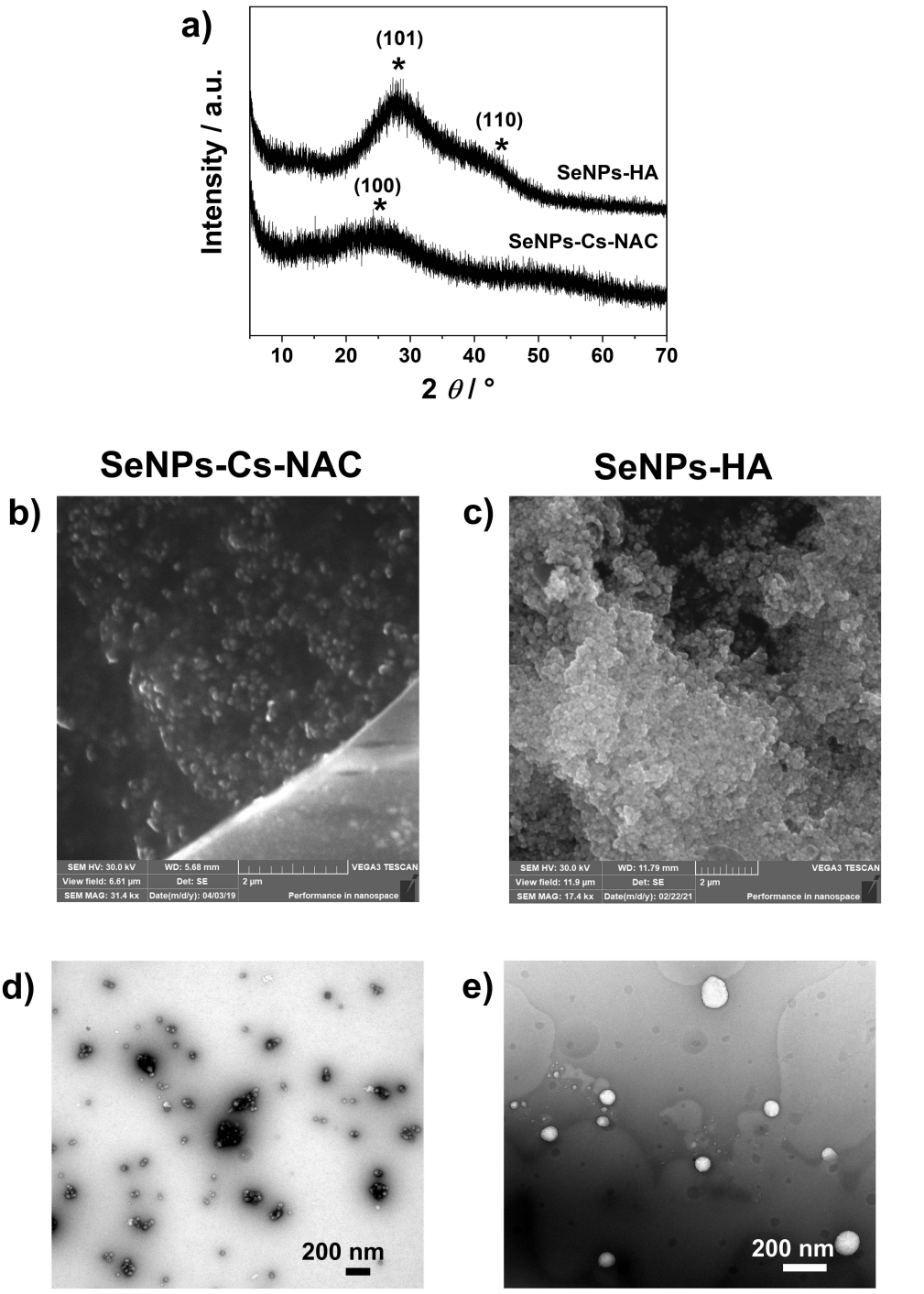

Figure 2 Characterization of SeNPs coated with Cs-NAC and HA. (**a**) PXRD diffraction patterns of SeNPs-Cs-NAC and SeNPs-HA. SEM images of (**b**) SeNPs-Cs-NAC and (**c**) SeNPs-HA; the scale bar represents 2 µm. TEM images of negatively stained and air-dried (**d**) SeNPs-Cs-NAC and (**e**) SeNPs-HA; the scale bar represents 200 nm.

to enhance the bioavailability of poorly water-soluble drugs, leading to amorphous solid dispersions.[45] Moreover, amorphous NPs have currently attracted significant interest in the pharmaceutical field due to their ability to enhance dissolution rates and increase supersaturation levels.[46] Based on these findings, the administration of amorphous SeNPs, as fabricated in this study, could be more beneficial for the absorption in GIT compared to crystalline forms.

SEM was employed to determine the morphology of lyophilized SeNPs-Cs-NAC/-HA. The SEM micrographs (Figure 2b and c) revealed dense, irregular spherical shapes for both types of SeNPs.

The sizes of SeNPs-Cs-NAC are in the range from 80 to 145 nm, while SeNPs-HA have a size distribution between 70 to 110 nm (n = 50). It is well established that SeNPs can take various shapes depending on the preparation conditions and solvents used for their synthesis.[47,48] Given that the preparation parameters for HA and Cs-NAC coated SeNPs produced here were essentially the same, the different morphologies observed in the SEM images are most likely due to interactions between SeNPs and the polymers, as well as interactions among individual polymer chains. When the lyophilized SeNPs-Cs-NAC/-HA were re-dissolved in MQ-water and visualized by TEM both types of particles showed spherical structures of different sizes (Figure 2d and e). The SeNPs exhibited sizes from 30–80 nm (n = 30), while the SeNPs-HA displayed sizes in the range from 50–150 nm (n = 30). In the work of Derakhshan-sefidi et al the sizes of SeNPs coated with Cs-cysteine coupled with nisin were between 90 and 180 nm.[49] Similar results were observed in the study of Zou et al where the SeNPs-HA loaded with paclitaxel exhibited spherical particles with diameters from 60 nm to 90 nm.[8]

Furthermore, DLS and ELS were employed to determine the particle size distribution and the zeta potential of SeNPs-Cs-NAC/-HA as important parameters to assess particle stability (Table 1). The hydrodynamic diameters, d_h, of SeNPs-Cs-NAC/-HA after dialysis in MQ-water were 146.4 ± 7.5 nm and 151.6 ± 4.0 nm, respectively (n = 6). The zeta potential values (ζ) of SeNPs-Cs-NAC/-HA in MQ-water were 17.7 ± 0.3 mV and –44.5 ± 1.1 mV, respectively (n = 3). The particle sizes of SeNPs-Cs-NAC/-HA after lyophilization and reconstitution were only slightly different, 141.8 ± 8.0 nm and 154.3 ± 4.7 nm, respectively (n = 6). The changes in the zeta potential were also minor with ζ = 21.3 ± 0.3 mV and –44.1 ± 1.4 mV for SeNPs-Cs-NAC/-HA, respectively (n = 3). Accordingly, neither the addition of mannitol nor the lyophilization process had a pronounced effect on the size and the zeta potential of SeNPs-Cs-NAC/-HA. The data also indicated that the SeNPs-Cs-NAC/-HA are in a size range commonly used for oral applications[50] and the particles were stable and could be stored as powder formulations at 25 °C for 12 months without any noticeable disadvantages.

Recognizing the importance of the surface charge for the interaction of NPs with biological components, we aimed to fabricate SeNPs with opposite surface charges as indicated in the zeta potential measurements. The notably high positive zeta potential observed for SeNPs-Cs-NAC can be attributed to the fact that Cs-NAC has a positive charge even at higher pH values due to the protonation of amino -groups.[51] In contrast, when the SeNPs were coated with HA and measured at pH > 3, the degree of the ionization of HA was increased, leading to negatively charged SeNPs.[52] Consequently, the surface charge of SeNPs can be effectively tailored through the surface chemistry of the polymers, thereby influencing the interaction with biological components within the body. As an example, NPs with a higher positive surface charge achieved by coating with higher molecular weight Cs revealed a stronger affinity to negatively charged cell membranes leading to an enhanced cellular uptake.[53] Additionally, the behavior of NPs in the presence of biological fluids may differ significantly from their behavior in water.

Protein Corona Formation

To investigate the effects of the gastric proteins, pepsin and pancreatin on the stability of the SeNPs-Cs-NAC/-HA, the particles were incubated with SGF/SIF as well as with enzyme-free SGF_0/SIF_0 for different lengths of time. To simulate oral digestion in the stomach and intestine, the selected incubation times were 30 minutes for SGF_0/SGF (pH 1.2) and 2 hours for SIF_0/SIF (pH 6.8), respectively. As summarized in Figure 3a and b, both the size and the zeta potential of

Table 1 Size (D_h) and Zeta Potential (ζ) of SeNPs Functionalized with Cs-NAC and HA After Synthesis (AS) and After the Lyophilization (AL) at 25 °C. n (Size Measurement) = 6 and n (Zeta Potential Measurements) = 3

NP Type	d_h / nm	ζ / mV
SeNPs-Cs-NAC (AS)	146.4 ± 7.5	17.7 ± 0.3
SeNPs-Cs-NAC (AL)	151.6 ± 4.0	21.3 ± 0.3
SeNPs-HA (AS)	141.8 ± 8.0	–44.5 ± 1.1
SeNPs-HA (AL)	154.3 ± 4.7	–44.1 ± 1.4

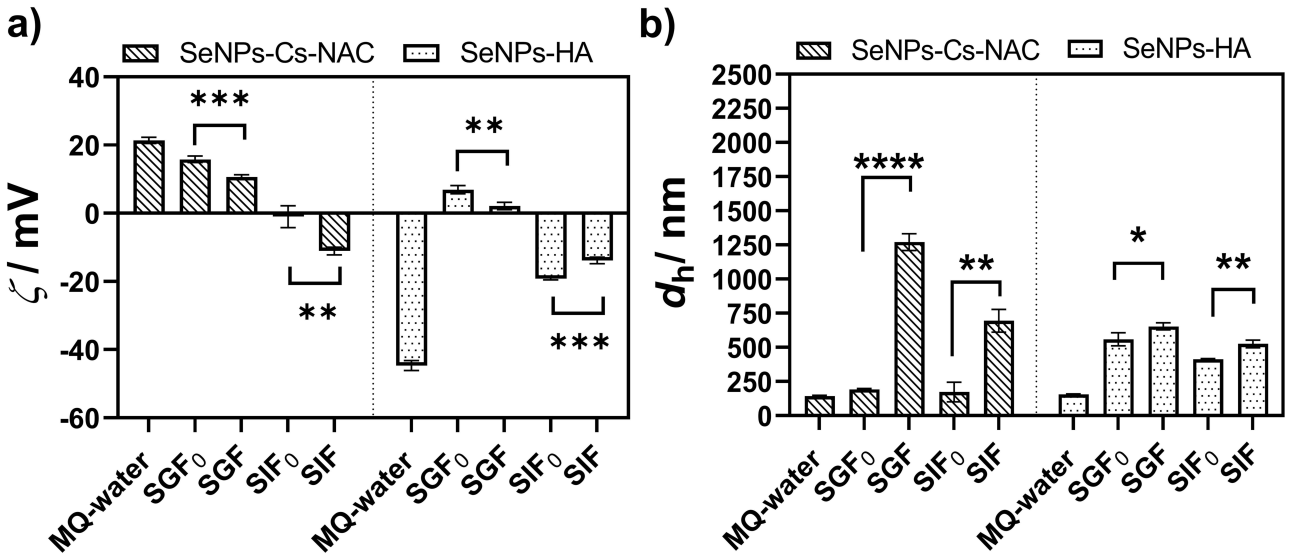

Figure 3 Protein Corona formation. (**a**) Zeta potential (ζ) and (**b**) hydrodynamic diameter (d_h) of SeNPs, functionalized with Cs-NAC or HA before and after incubation in enzyme-free simulated gastric fluid (SGF_0), enzyme-free simulated intestine fluid (SIF_0), simulated gastric fluid (SGF) and simulated intestine fluid (SIF). γ(SeNPs) = 250 mg/L (n = 3). An unpaired *t*-test was performed, and statistical significance was assigned as * $p < 0.05$, ** $p < 0.01$ and *** $p < 0.001$, **** $p < 0.0001$ where p-value <0.05 was considered statistically significant.

both types of SeNPs, underwent substantial changes. When SeNPs-Cs-NAC were incubated with enzyme-free media (SGF_0/SIF_0) to assess the impact of pH and ionic strength on the stability, a decrease in the zeta potential values from 21.4 mV to 15.8 mV in SGF_0 and to −0.19 mV in SIF_0 were observed, while the size increased to 192.9 nm in SGF_0 and 173.4 nm in SIF_0. The effects on SeNPs-HA were even more pronounced. The particle size in SGF_0 and SIF_0 changed from 154.3 nm in MQ-water to 559.1 nm and 412.9 nm in SGF_0 and SIF_0, respectively. The zeta potential changed from –44.67 mV in MQ-water to 6.90 mV in SGF_0 and –19.20 mV in SIF_0. According to these data, the stability of SeNPs-HA is strongly impaired, and the particles are prone to agglomeration. It can be assumed that this instability is due to the combined influence of pH (1.2 and 6.8) and ionic strength (0.097 M in SGF_0 and 0.064 M in SIF_0). A similar impact on the stability of SeNP including the influence of the surface chemistry of the coating agent was recently reported by Borowska et al[54]

The addition of gastric enzymes further affected the zeta potential and particle size of SeNPs-Cs-NAC/-HA. When SeNPs-Cs-NAC were incubated in SGF (pepsin-containing solution; ζ = 2.36 ± 0.70 mV), the zeta potential dropped from 15.8 mV in SGF_0 to 10.6 mV in SGF, and agglomerates larger than 1 µm were detected. A similar behavior was observed in SIF (pancreatin-containing solution; ζ = –12.45 ± 0.46 mV), where the surface charge of SeNPs-Cs-NAC became more negative (ζ = –11.1 mV) than after incubation in SIF_0 (ζ = –0.19 mV), followed by an increase in NP size to (d_h = 695.3 nm). The large shift in the hydrodynamic diameter compared to the particle size after incubation in SGF_0 /SIF_0 is a strong indication for the adsorption of pepsin/pancreatin on the surface of SeNPs-Cs-NAC but also for an increased tendency of SeNPs-Cs-NAC to agglomerate. In the case of SeNPs-HA, a similar trend was noticed, whereas the presence of gastric enzymes further contributed to particle destabilization. The zeta potential of SeNPs-HA changed from 6.9 mV to 2.1 mV, and the size from 559.1 nm to 653.8 nm after incubation with SGF, indicating that pepsin adsorbed onto the surface of SeNPs-HA. Similarly, the incubation with SIF led to an increase in zeta potential from –19.2 mV to –13.9 mV and an increase in particle size for approximately 100 nm when compared to the size in SIF_0 (d_h = 412.9 nm). The pronounced changes in size and zeta potential observed after incubation with gastric fluids as well as the formation of agglomerates could be explained by the altered surface charge and conformation of the polymers due to exposure to high ionic strength, which hinders electrostatic repulsions. In addition, the adsorbed proteins could bridge individual SeNPs, thus fostering agglomeration by crosslinking NPs, ultimately leading to the formation of larger clusters.[55]

A similar behavior was reported by Peng et al, who investigated the interaction between the poly(3-hydroxybutyrate-co-3-hydroxyhexanoate)-based cationic NPs (CNPs) and pepsin and pancreatin.[56] They demonstrated that both proteins adsorbed onto the surface of CNPs, resulting to agglomeration. Likewise, Borowska et al reported that the adsorption of pepsin onto yeast extract-coated SeNPs also promoted agglomeration.[54]

To further investigate the structure of SeNPs-Cs-NAC/-HA and changes upon incubation with gastrointestinal proteins, FTIR spectroscopy was utilized. FTIR spectra of SeNPs-Cs-NAC/-HA, pure pepsin, and pancreatin, which served as control, as well as SeNPs-Cs-NAC/-HA in the presence of pepsin/pancreatin are presented in Figure 4a and b. The FTIR spectra of SeNPs-Cs-NAC/-HA demonstrated peaks at 563 cm^{-1} and 511 cm^{-1} respectively, along with a peak at 774 cm^{-1} corresponding to Se-O stretching vibration (Figure 4a and b, Tables S1 and S2). The vibrations can be attributed to the binding of the SeNPs to the carbonyl groups of HA and Cs-NAC that coat SeNPs. Similar observations have been demonstrated previously with oxidized products of ascorbic acid.[57,58] Specific differences of SeNPs-Cs-NAC/-HA can be noticed in the region 1700 cm^{-1} - 900 cm^{-1} (Figure 4a and b, Tables S1 and S2). In the SeNPs-Cs-HA spectra specific peaks were obtained at 1210 cm^{-1} corresponding to COO− stretching and a single peak at 1039 cm^{-1} corresponding to CH stretching. Those peaks have not been observed in the SeNPs-Cs-NAC spectra. Furthermore, in the SeNPs-Cs-NAC spectra specific peaks at 1153 cm^{-1} and 1067 cm^{-1} correspond to C−O−C and C−O stretching were observed.[59] The presence of specific peaks suggests that the SeNP' surface was coated with the investigated polymers.

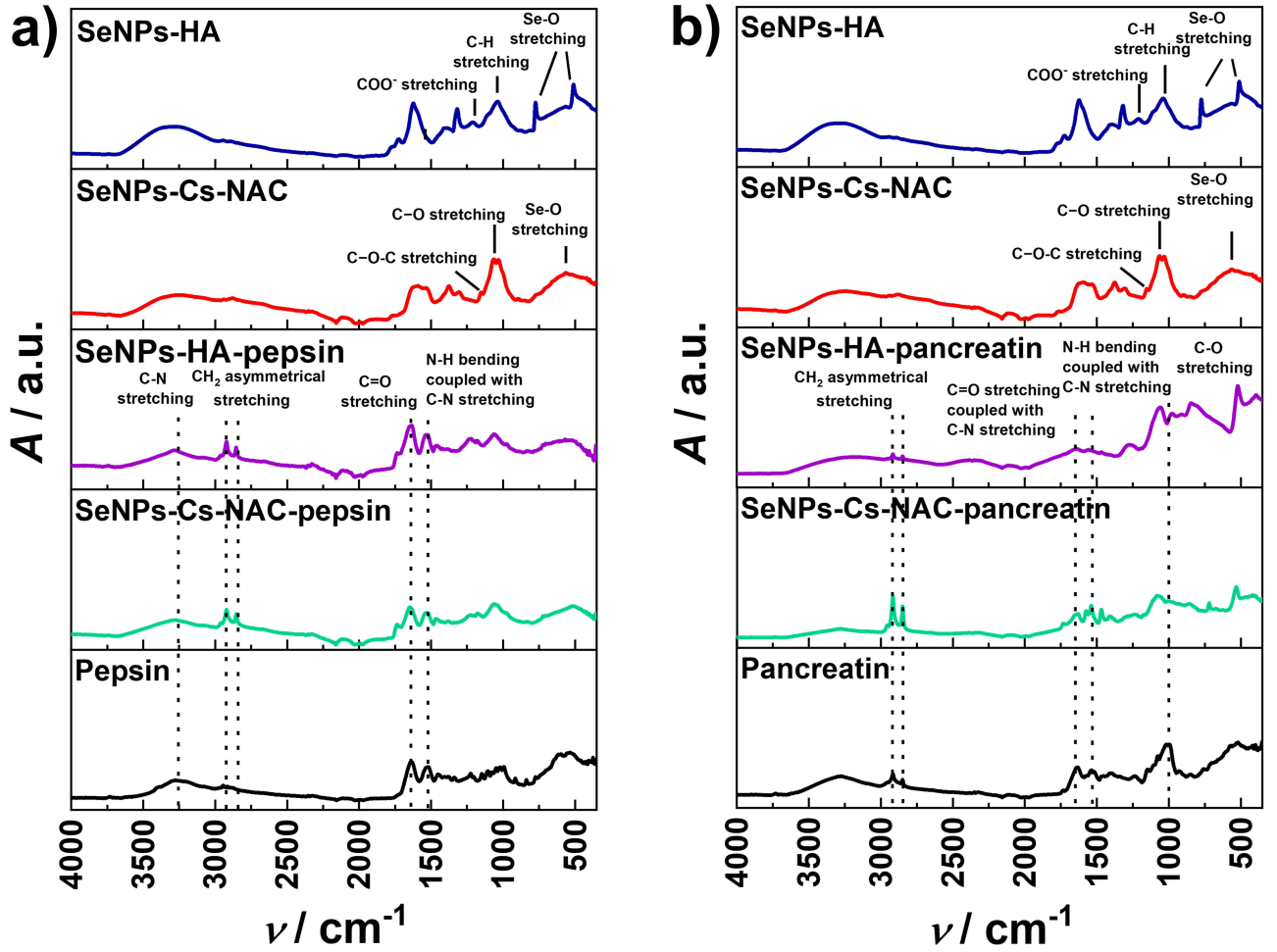

Figure 4 FTIR spectra of SeNPs coated with Cs-NAC or HA incubated in (**a**) SGF_0/SGF: (—) pepsin in SGF, (—) SeNPs-Cs-NAC in SGF_0, (—), SeNPs-Cs-NAC in SGF, (—) SeNPs-HA in SGF_0, (—) SeNPs-HA in SGF and (**b**) SIF_0/SIF: (—) pancreatin in SIF, (—) SeNPs-Cs-NAC in SIF_0, (—), SeNPs-Cs-NAC in SIF, (—) SeNPs-HA in SIF_0, (—) SeNPs-HA in SIF.

The FTIR spectra of pepsin (Figure 4a, Table S3) showed the presence of strong peaks at 3273 cm^{-1} corresponding to C−N stretching, 2943 cm^{-1} corresponding to CH_2 asymmetrical stretching and, 2914 cm^{-1} and 2891 cm^{-1} corresponding to CH_2 symmetrical stretching. In the 1600−1700 cm^{-1} range a peak was noticed corresponding to the C=O stretching vibrations and hydrogen bond coupled with CN stretch, and in the amide II region a peak at 1520 cm^{-1} corresponding to the NH bend coupled with CN stretching was observed.[24,26] Compared to pure spectra of SeNPs-Cs-NAC/HA after incubation in the SGF additional vibration peaks appeared, namely sharp peaks at 2915 cm^{-1}, 2850 cm^{-1}, wide peaks at 1640 cm^{-1} and 1524 cm^{-1} (Figure 4a). Since the SeNPs-Cs-NAC/-HA were washed after the incubation with pepsin to remove unbound protein from the surface of the SeNPs, the results indicate pepsin binding to the surface of the SeNPs.

For pure pancreatin (Figure 4b, Table S3) measured in the same regions, the most pronounced peaks were observed at 2918 cm^{-1} and 2846 cm^{-1} corresponding to CH_2 symmetrical stretching, 1625 cm^{-1} corresponding to C=O stretch and hydrogen bond coupled with CN stretch, 1524 cm^{-1} corresponding to NH bend coupled with CN stretch, and 1017 cm^{-1} corresponding to C−O stretching vibrations.[60,61] Compared to pure spectra of SeNPs-Cs-NAC/HA after incubation in the SIF additional vibration peaks appeared, namely sharp peaks at 2954 cm^{-1}, 2918 cm^{-1}, 2846 cm^{-1}, a wide peak at ≈ 1636 cm^{-1} and a wide peak at 1266 cm^{-1} which was shifted compared to pure pancreatin and NAC/HA. Again, the unbound protein was washed away before the spectra were recorded, indicating pancreatin binding to the surface of the SeNPs.

From the FTIR results it can be concluded that both pepsin and pancreatin interact with both types of SeNPs as seen by the presence of the additional characteristic protein peaks in the spectra of SeNPs-Cs-NAC/-HA after incubation with SGF/SIF.

Determination of Binding Affinity of Gastric Proteins for SeNPs

QCM-D was used to study the interaction between SeNPs-Cs-NAC/-HA and gastric proteins in more detail. QCM-D enables in-situ monitoring of the interaction between NPs and functionalized substrates, proteins, antibodies, etc. Changes in the Δf and the ΔD can be correlated with adsorption/desorption processes and viscoelastic properties, respectively.[62] When SGF/SIF was introduced in QCM-D, the frequency decreased, and the dissipation factor increased (Figure 5a-d). Both proteins, either pepsin or pancreatin, were adsorbed on the Au sensor due to the formation of bonds with thiol residues present on the protein surfaces.[25] Frequency shifts were of the order of 50 hz, amounting to full coverage with about 10 nm of biomaterial of $1 g/cm^3$ density, according to a Sauerbrey equation for rigid layers. It is to be noted that the behavior of ΔD parameter is symmetric to the behavior of Δf, which indicates similar viscoelastic properties of all the deposited layers, presumably rather compact and formed by well-bound particles. The enzymes were rather strongly bound as the positive frequency shift and the decrease of the dissipation factor was minimal after the washing step with enzyme-free SGF_0/SIF_0. That is, about 20% of protein mass was adsorbed, but no bonds were formed and it was removed. Only a limited amount of SeNPs was deposited (Δf~ 5 hz) in the case of pepsin (from SGF) functionalized surface. This amount was considerably smaller than for SIF (pancreatin - trypsin, amylase, and lipase) treated surface (Δf ~ 20–40 hz), independently of the particle type (SeNPs-Cs-NAC vs SeNPs -HA). Overall, the SeNPs bind to the gastric proteins (pepsin/pancreatin) modified Au sensor and are not removed by the washing step with enzyme-free SGF_0/SIF_0. In the case of quantitative removal upon washing, we would expect the recovery of the Δf that corresponds to Δf before the addition of SeNPs.

Notably, the deposition of Se-NPs on the Au-surface beneath the protein layer is not due to thiol binding. Instead, the likely mechanism involves the binding of the NPs to the protein layer itself. This conclusion is supported by the observation that the binding affinity is independent of the type of nanoparticle (SeNPs-Cs-NAC vs SeNPs-HA) and is instead determined by the proteins present on the surface (pepsin or pancreatin).

To quantify the affinity of pepsin and pancreatin for SeNPs-Cs-NAC/-HA, fluorescence quenching titration was applied. Changes in the fluorescence spectra represent the changes in the intrinsic fluorescence of tryptophan (Trp) residues in pepsin and pancreatin, therefore changes in the microenvironment around the Trp upon adding SeNPs-Cs-NAC/-HA were investigated. The results of the concentration-dependent decrease (quenching) of the Trp fluorescence signal with increasing concentrations of SeNPs are presented in Figure 6a-d. As presented, there were no obvious shifts in the maximum emission wavelengths of pepsin and pancreatin, suggesting that the Trp microenvironment was not altered by the addition of SeNPs-Cs

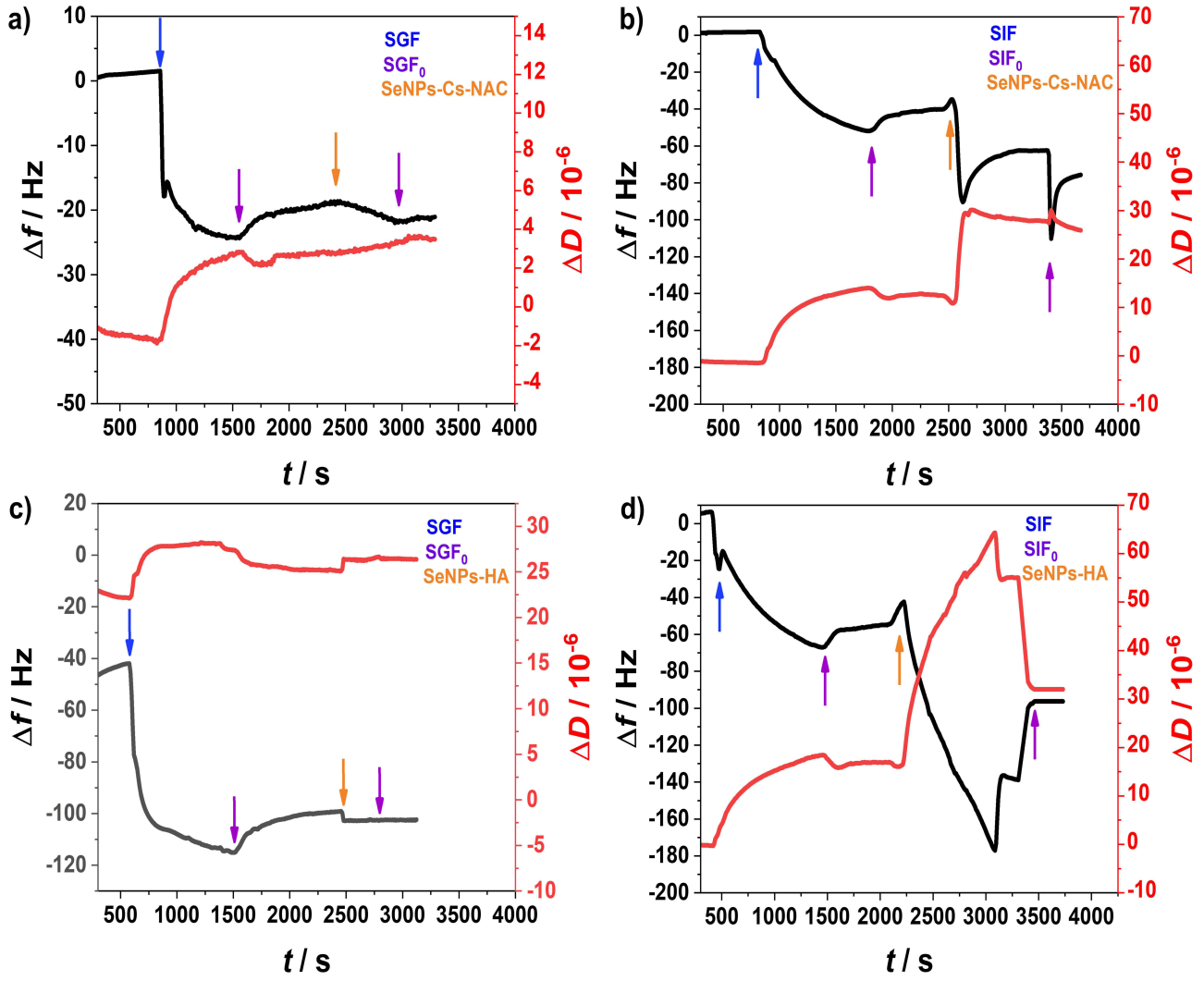

Figure 5 QCM-D in-situ monitoring of the interaction between SeNPs and proteins. Frequency shift and dissipation of energy. (**a**) SeNPs-Cs-NAC in SGF, (**b**) SeNPs-Cs-NaC in SIF, (**c**) SeNPs-HA in SGF, (**d**) SeNPs-HA in SIF. (—) f_3 denote the overtone and (—)ΔD_3 the corresponding dissipation of energy. The arrows show the time points for the addition of (↑) SGF/SIF, (↑) SGF_0/SIF_0, and (↑) SeNPs-Cs-NAC/-HA.

-NAC/-HA. The apparent equilibrium dissociation constants (K_D) were determined from the fluorescence titration curves (Figure 7 and Table 2). The K_D constants revealed that pepsin and pancreatin have a higher affinity for SeNPs-Cs-NAC than for SeNPs-HA, which displayed higher equilibrium dissociation constants upon interaction with pepsin and pancreatin.

The K_D values align well with the size data, demonstrating that the impact of Cs-NAC on the physicochemical properties of SeNPs is more pronounced compared to HA. This higher affinity can be attributed to the structure of Cs-NAC, which contains free thiol groups capable of forming covalent disulfide bonds with cysteine residues in pepsin and pancreatin.[63] Furthermore, the extent of the interaction between gastric proteins and SeNPs must also be correlated with previously mentioned parameters like pH, and ionic strength as well as with the concentration of the SeNPs and the incubation time due to their delicate interplay that could direct or interfere with the final fate of NPs upon administration.

Radical Scavenging Potential

Nutritive supplements that exhibit anti-oxidative properties can alleviate the risk of many health conditions. They have a protective role by neutralizing free radicals that are involved in the initiation of oxidative processes. So far, the anti-oxidative benefits of SeNPs have been shown in numerous studies.[64–66] Here, the DPPH assay was applied to determine the anti-oxidative potential of SeNPs-Cs-NAC/-HA in terms of free radical scavenging (FRS) ability. The DPPH assay is

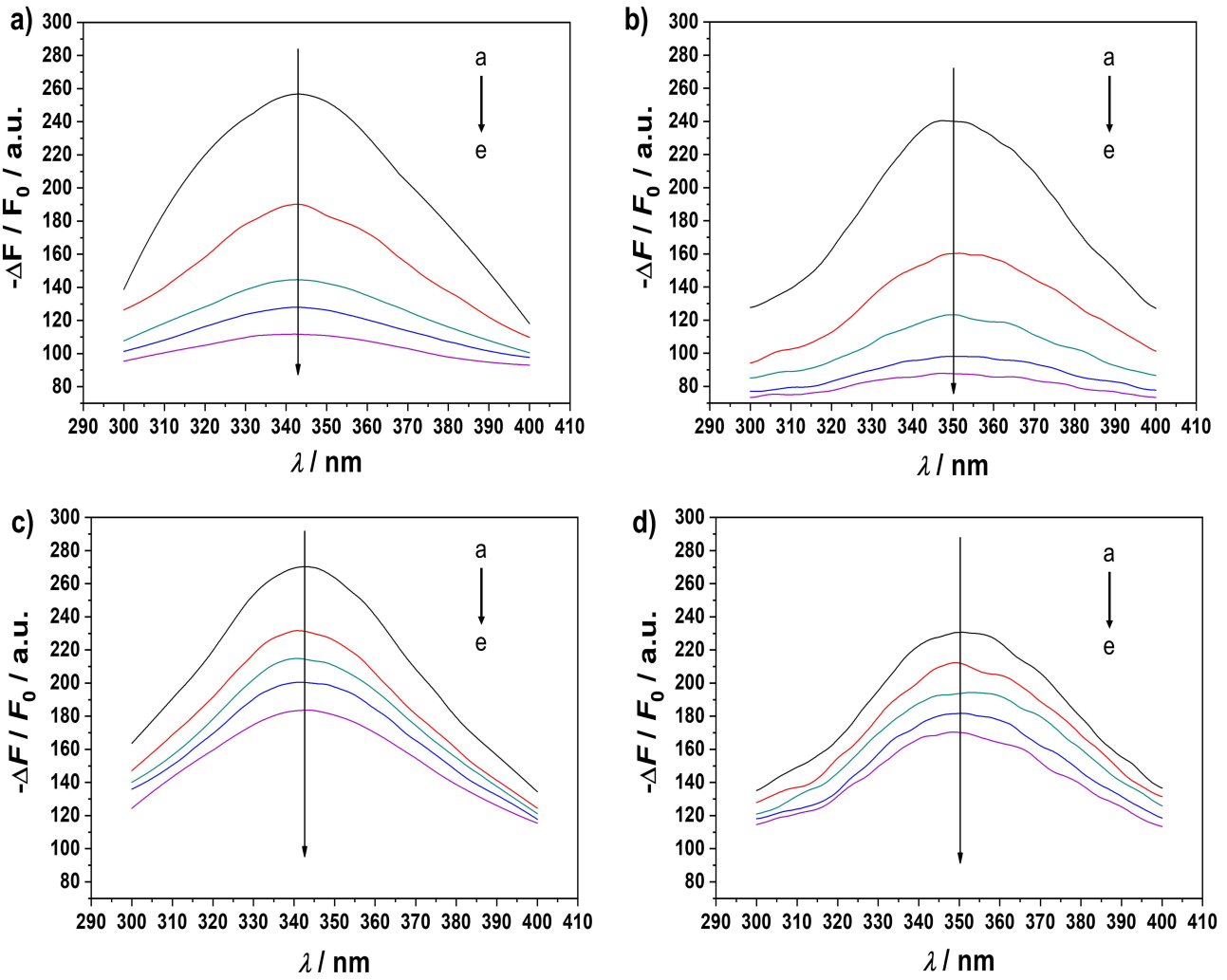

Figure 6 Fluorescence emission spectra obtained for (**a**) pepsin in SGF and (**b**) pancreatin in SIF incubated with various concentrations of SeNPs-Cs-NAC, (**c**) pepsin in SGF and (**d**) pancreatin in SIF incubated with various concentrations of SeNPs-Cs-HA. SeNPs-Cs-NAC/-HA concentrations (a-e): (—) 0, (—) 500, (—) 1000, (—) 1500 and (—) 2000 μM.

based on the change in the absorbance of DPPH radicals upon incubation with antioxidants. The stable nitrogen radical becomes inactivated by the exchange of hydrogen, which leads to the corresponding hydrazine production ($DPPH_2$).[67] The ascorbic acid that served as the positive control exhibited the free radical scavenging potential of 50.2% and 93.5% using concentrations of 1 mm and 10 mm ascorbic acid, respectively. The antioxidative potential of both types of SeNPs is presented in Figure 8. The FRS potential of SeNPs-Cs-NAC/-HA increased with concentration from 10 to 100 mg/L of SeNPs. For SeNPs-Cs-NAC, the FRS increased notably from 2.3 to 29.0%, while for SeNPs-HA, the increase was from 4.6 to 28.1%. Thus, both types of SeNPs displayed similar anti-oxidative potential that could be attributed to the contribution of the polymers. The proposed reactions involved in the antioxidative mechanism are hydrogen abstraction, addition reaction, or electron transfer.[68] The free radical scavenging potential of Cs and its derivatives may be ascribed to the reaction between free amino and hydroxyl groups in the chitosan unit and the free radical. Additionally, NAC has known antioxidative properties and the action mechanism could be via the interaction of free thiol groups with free radicals.[69]

HA also has an antioxidative capacity, especially when grafted on NPs surfaces where the hydrogen-atom transfer is the driving force for the antioxidative behavior.[70,71] To sum up, the antioxidative potential of SeNPs-Cs-NAC/-HA could be beneficial for the development of SeNPs as the nutraceutical with a dual role that mitigates Se deficiency and immune

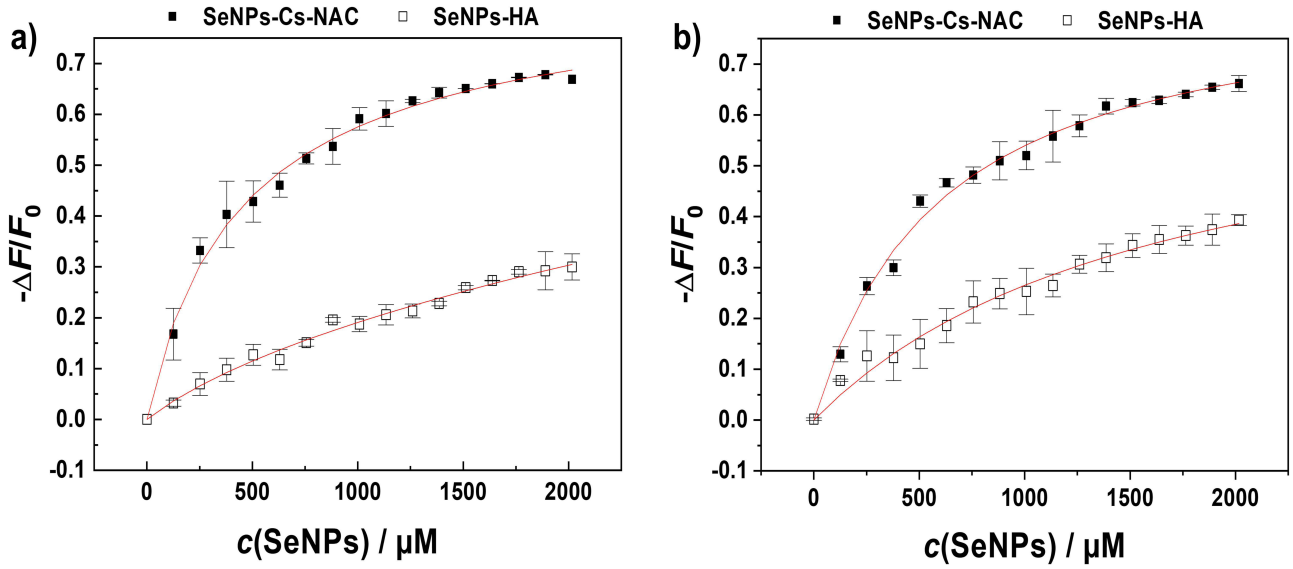

Figure 7 Fluorescence titration curves of SeNPs-Cs-NAC (■) and SeNPs-HA (□) binding to (**a**) pepsin. and (**b**) pancreatin. The data represent mean ± SD (n = 3). The change in the fluorescence intensity (Δ*F*) upon adding SeNPs was calculated by subtracting the intrinsic fluorescence intensity of the protein (F_0) at the emission maximum from the maximal intensity value recorded at a given SeNP concentration. The data are normalized by dividing by the intrinsic fluorescence of the protein (F_0).

response and simultaneously exhibits re-inforced antioxidative potential due to a synergism between SeNPs and biocompatible coating agents like Cs-NAC and HA.

Discussion

SeNPs are a class of nanoparticles that have emerged as promising nutritional supplements for Se, a vital element that plays a critical role in various physiological processes in the human body. Se deficiency has been linked to numerous serious health conditions caused by insufficient Se intake. In this study, SeNPs coated with two different biocompatible polymers, Cs-NAC and HA, were specifically synthesized for oral drug administration. The stability of these coated SeNPs was assessed in simulated gastric fluids (SGF/SIF) in the absence and presence of major gastric proteins, pepsin and pancreatin, with DLS and ELS measurements. The size of SeNPs-Cs-NAC increased slightly in SGF_0/SIF_0, while the size of SeNPs-HA increased dramatically (by 3–4 times), primarily due to aggregation. This increase in particle size was accompanied by a decrease in zeta potential for both types of SeNPs. It has to be considered that the surface chemistry of the coating agent is itself affected by the pH and the presence of electrolytes in the solutions.[72,73] At low pH, Cs-NAC contains protonated positively charged amino and neutral thiol groups. Since only 4.3% of the total amino groups are thiolated, 95.7% of the amino groups remain available for further interactions. These available protonated amino groups cause repulsion between the positively charged units. At a pH of 6.8 (SIF_0), the neutral amino-groups start to

Table 2 The Apparent Equilibrium Dissociation Constants Between SeNPs Coated with Cs-NAC or HA and Pepsin or Pancreatin. t = 25 °C. (n = 3)

Protein	NP Type	K_D/mM
Pepsin	SeNPs-Cs-NAC	0.45 ± 0.02
	SeNPs-HA	2.51 ± 0.41
Pancreatin	SeNPs-Cs-NAC	0.59 ± 0.04
	SeNPs-HA	1.61 ± 0.24

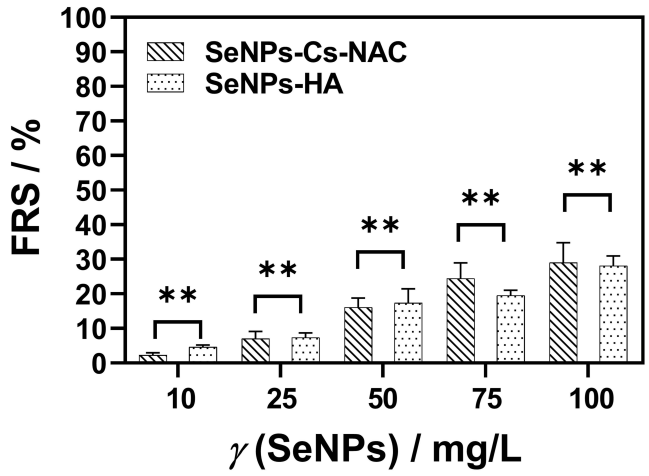

Figure 8 Free radical scavenging (FRS) potential of Cs-NAC and HA-coated SeNPs. The values of FRS are expressed as mean values ± SD (n = 3). An unpaired *t*-test was performed, and statistical significance was assigned as ** $p < 0.01$ where a p-value <0.05 was considered statistically significant.

predominate as the pK_a of the amino groups in Cs-NAC is 6.5. The pK_a of thiol groups in NAC is 9.5 and the SH groups remain protonated and uncharged at pH 6.8.[74] As a result, at pH 6.8 the key functional groups on the polymer chain are mostly neutral and the polymer adopts a more compact conformation, which causes instability of SeNPs-Cs-NAC. Apart from pH, the ionic strength of SGF_0/SIF_0 plays a critical role. At low pH, such as in the stomach, Cs-NAC behaves as a polycation and the polymer units repel each other. However, an increase in the ionic strength and the presence of counterions from electrolytes can shield the charges on the amino groups disrupting the extended polymer structure. Thus, the repulsion between the polymer chains is reduced leading to instability and particle agglomeration as observed in the size measurements. In the intestine where the pH is higher, deprotonation of amino groups reduces the overall positive charge making the polymer structure more compact due to diminished electrostatic repulsion. The combination of amino group deprotonation and high ionic strength results in a more rigid structure of the polymer chains, ultimately promoting aggregation.

In the case of HA, an acidic medium such as SGF_0 induces a more compact conformation of HA due to the protonation of carboxylic groups, which diminishes the stabilization effect on the NPs. At higher pH values, the ionization of the polymer is increased, causing negatively charged polymer units to repel each other, thereby enhancing NP stability. However, the high ionic strength of the tested medium disrupts the stability of HA leading to aggregation. In SIF_0, HA behaves as a polyanion due to the deprotonated carboxyl groups. However, the high ionic strength shields the negative charges thus adversely affecting the stability of the polymer. In summary, as ionic strength increases, counterion condensation becomes more pronounced, affecting polymer conformation and decreasing NP stability, as demonstrated by size and zeta potential measurements.[75]

When SeNPs-Cs-NAC/-HA were incubated in SGF/SIF, the adsorption of gastric proteins onto the SeNP surfaces significantly impacted their stability compared to SGF_0/SIF_0 due to the formation of a PC. Notably, the changes in size and zeta potential were particularly pronounced for SeNPs-Cs-NAC where particle sizes larger than 1 μm were observed in SGF. Besides pH and ionic strength, which affect the polymer surface chemistry, the proteins possess multiple binding sites acting as crosslinker. These protein bridging interactions may overcome the electrostatic repulsion between NPs due to the physiological media screening effects (pH and the salt composition).[76]

To further investigate the PC formation, the adsorption and binding behaviour of the proteins on the surface of SeNPs were studied by QCM-D and fluorescence quenching spectroscopy. The data indicated that both pepsin and pancreatin bind to the surface of SeNPs in a manner dependent on the coating agent. SeNPs coated with Cs-NAC showed a higher affinity for pepsin and pancreatin compared to those coated with HA. Protein-NP interaction is a dynamic process in which both protein adsorption and desorption occur simultaneously.[77] The driving forces that govern the adsorption of proteins on NP surfaces could be electrostatic, van der Waals, covalent, steric, or hydrophobic interactions. Depending on

the type of interaction, some of the adsorbed proteins are attached tightly (hard corona), while others are more loosely attached forming a soft corona.[78]

The differences in how pepsin and pancreatin interact with SeNPs-Cs-NAC/-HA can be explained by the structure of the polymer. The binding module between Cs and proteins is established through electrostatic interactions between amino groups of Cs and the acidic amino acids in proteins.[63] In addition, the conjugation of Cs with NAC led to the introduction of free SH-groups in the Cs polymer units that could interact with the cysteine residues present in pepsin and pancreatin, thus forming covalent disulfide bonds. Conversely, the polymer unit of HA has a carboxylic group that is protonated or deprotonated, depending on the pH resulting in weaker electrostatic and van der Waals interactions compared to disulfide bonds. This difference could explain why the interaction between proteins and SeNPs-Cs-NAC is stronger, as seen by the fluorescence measurement.

Such differences in the binding affinity of gastric peptides to SeNPs could significantly impact the activity of SeNPs when administered orally as a nutritive supplement for the mitigation of Se deficiency. The SeNPs-Cs-NAC in the SGF_0 showed better stability compared to SeNPs-HA. This suggests that SeNPs-Cs-NAC remain more stable in the acidic environment of the stomach, which is crucial for maintaining the bioavailability. Cs-NAC coated SeNPs exhibited stronger interactions with gastric proteins (pepsin and pancreatin), as evident from the lower apparent equilibrium dissociation constants, compared to SeNPs-HA. This stronger interaction may promote the formation of a protective protein corona around SeNPs-Cs-NAC, potentially enhancing their stability and absorption in the stomach. The structure of Cs-NAC, particularly its free thiol groups, enables it to form covalent disulfide bonds with cysteine residues in proteins such as pepsin and pancreatin. This could help protect SeNPs from degradation, further supporting their bioavailability in the gastric environment. In contrast, SeNPs-HA demonstrated a higher tendency to aggregate in the tested media, which could lead to reduced bioavailability. Despite the differences in protein interactions, both types of SeNPs exhibited similar radical-scavenging potential, an important factor in developing nutritional supplements that can mitigate the risk of various health conditions. The polymer coated SeNPs ensure that SeNPs remain in their active, reduced state. This is crucial for the preservation of antioxidative properties allowing sustained and controlled release of Se. The intrinsic antioxidative properties of SeNPs are reinforced by Cs-NAC and HA, both of which also display antioxidative potential. It was shown that SeNP supplementation promotes the growth of gut microbiota and associated metabolic pathways by the growth enhancement of beneficial bacteria such as *Bifidobacterium* and *Lactobacillus*.[79,80] However, gut health and its barrier function could be disrupted by opportunistic bacteria, and oxidative stress can damage the gut lining and affect microbial composition. SeNPs play a preventive and protective immunomodulatory role by regulating cytokine production (promoting anti-inflammatory cytokines while reducing pro-inflammatory ones), immune cell activity, and mediating the immune response. Functionalizing SeNPs with Cs-NAC and HA could impact the intestinal barrier function, gut microbiota and immune response. The particles could potentially be optimized to develop personalized treatments tailored to an individual's microbiome profile, thereby improving gut health and immune resilience. However, even if the physicochemical properties of engineered NPs are optimized to the highest extent, the biological milieu and its complex composition might alter the surface properties of the NPs and affect their primary designated application.[14,81] Besides the impact of the adsorbed proteins on NP's internalization into the cells, this interaction might also alter the conformation of the adsorbed protein leading to impaired enzyme function that could trigger an immune response or impact cell signaling relevant to therapeutic applications.[82,83] For example, the binding of GI proteins, namely pepsin, α-amylase, and trypsin, onto polystyrene nanoparticles reduced their activity, as presented in the study of Wang and co-workers.[23] In another study, the microenvironment of the aromatic amino acids of pepsin in the presence of titanium oxide nanoparticles was altered upon PC formation affecting pepsin activity.[25] Consequently, it remains an important issue to study the interaction of NPs with GI proteins in greater detail to predict possible events that could occur upon NP administration and to estimate the fate of NPs in the microenvironment of the GIT.

Conclusion

This study highlights the critical role of the protein corona on the stability and surface characteristics of Cs-NAC or HA functionalized SeNPs under simulated gastrointestinal conditions. Variations in pH and ionic strength led to agglomeration of SeNPs, with the extent of agglomeration strongly dependent on the physicochemical properties of the coating

polymer. The binding of gastric proteins to SeNPs further altered their particle size and zeta potential leading to increased instability. In-situ adsorption measurements and fluorescence quenching titration experiments revealed that both pepsin and pancreatin had a binding affinity for SeNPs functionalized with Cs-NAC or HA. The affinity was notably stronger for SeNPs coated with positively charged Cs-NAC compared to those coated with slightly negatively charged HA. Such differences in the binding affinity of gastric peptides to SeNPs could markedly impact the activity of SeNPs when administered orally as nutritive supplement to address Se deficiency. Both Cs-NAC and HA functionalized SeNPs exhibited similar radical scavenging potential, which is important for supporting immune response and maintaining gut homeostasis after administration.

In summary, the interplay of NP polymer coating surface chemistry, pH, ionic strength, and protein binding dynamics highlights the importance of a rational design approach in developing SeNPs as nutraceuticals. A deeper understanding of these factors might contribute to advancements in personalized medicine, potentially ameliorating gut health and strengthening immune responses.

Abbreviations

SeNPs, selenium nanoparticles; Cs-NAC-thiolated, chitosan/chitosan-N-acetyl-cysteine; HA, hyaluronic acid; Se, selenium; GI, gastrointestinal; GIT, gastrointestinal tract; PC, protein corona; SGF, simulated gastric fluid; SIF, simulated intestine fluid; Cs, chitosan; CD44, cell surface adhesion receptor; TLR4, Toll-like receptor 4; SH, thiol group; FTIR, Fourier transform infrared; QCMD, quartz crystal microbalance with dissipation monitoring; Na_2SeO_3, sodium selenite; $NaHCO_3$, sodium bicarbonate; M_w, molecular weight; 1%; w/w, weight per weight percentage; DTNB, 5,5- dithiobis-2-nitrobenzoic acid; DPPH, 2,2-diphenyl-1-picrylhydrazyl; PBS, phosphate buffer; MQ-water, ultra pure Milli-Q water; % w/v, weight per volume percentage; SGF_0, simulated gastric fluid without added pepsin; SIF_0, simulated intestine fluid without added pancreatin; PXRD, powder X-ray diffraction; SEM, scanning electron microscopy; TEM, transmission electron microscopy; DLS, dynamic light scattering; ELS, electrophoretic light scattering; AT, angular cut.

Data Sharing Statement

Data will be made available on request.

Acknowledgments

A.S. thanks the Austrian Agency for International Cooperation in Education and Research (OeAD, ICM-2020-00205) and the Croatian Academy of Sciences and Arts for the financial support. ID and BR gratefully acknowledge financial support from the Center of Excellence for Advanced Materials and Sensing Devices, ERDF Grant No. KK.01.1.1.01.0001. and the Centre for Advanced Laser Techniques (CALT), co-funded by the European Union through the European Regional Development Fund under the Competitiveness and Cohesion Operational Programme (Grant No. KK.01.1.1.05.0001). The authors would like to express great thanks to Branimir Valenčak and Anton Paar (Croatia), who supported the size measurements.

Disclosure

Dr. Andreas Bernkop-Schnürch is the CEO of the company Thiomatrix®, which provided the thiolated chitosan (Cs-NAC), polymer used in the production of the thiolated chitosan functionalized selenium nanoparticles (SeNPs-Cs-NAC) in this study. This material contribution did not influence the study's design, data collection, analysis, or the interpretation of the results. The authors declare that the company did not have any involvement in the decision to publish the findings, and there are no other competing interests related to this work.

References

1. Labunskyy VM, Hatfield DL, Gladyshev VN. Selenoproteins: molecular pathways and physiological roles. *Physiol Rev*. 2014;94(3):739–777. doi:10.1152/physrev.00039.2013
2. Rayman MP. Selenium and human health. *Lancet*. 2012;379(9822):1256–1268. doi:10.1016/S0140-6736(11)61452-9

3. Zhang J, Saad R, Taylor EW, Rayman MP. Selenium and selenoproteins in viral infection with potential relevance to COVID-19. *Redox Biol*. 2020;37:101715. doi:10.1016/j.redox.2020.101715
4. Hosnedlova B, Kepinska M, Skalickova S, et al. Nano-selenium and its nanomedicine applications: a critical review. *Int J Nanomed*. 2018;13:2107–2128. doi:10.2147/IJN.S157541
5. Feng Y, Su J, Zhao Z, et al. Differential effects of amino acid surface decoration on the anticancer efficacy of selenium nanoparticles. *Dalton Trans*. 2014;43(4):1854–1861. doi:10.1039/C3DT52468J
6. Soares S, Sousa J, Pais A, Vitorino C. Nanomedicine: principles, properties, and regulatory issues. *Front Chem*. 2018;6. doi:10.3389/fchem.2018.00360
7. Tugarova AV, Kamnev AA. Proteins in microbial synthesis of selenium nanoparticles. *Talanta*. 2017;174:539–547. doi:10.1016/j.talanta.2017.06.013
8. Zou J, Su S, Chen Z, et al. Hyaluronic acid-modified selenium nanoparticles for enhancing the therapeutic efficacy of paclitaxel in lung cancer therapy. *Artif Cells Nanomed Biotechnol*. 2019;47(1):3456–3464. doi:10.1080/21691401.2019.1626863
9. Wang H, Wei YL, Liang XY, et al. Novel bilayer Pickering emulsions stabilized by in situ modification of zein via selenium nanoparticles: optimization, physicochemical properties and permeation. *Food Hydrocoll*. 2024;156:110323. doi:10.1016/j.foodhyd.2024.110323
10. Jha N, Esakkiraj P, Annamalai A, Lakra AK, Naik S, Arul V. Synthesis, optimization, and physicochemical characterization of selenium nanoparticles from polysaccharide of mangrove Rhizophora mucronata with potential bioactivities. *J Trace Elements Minerals*. 2022;2:100019. doi:10.1016/j.jtemin.2022.100019
11. Lou J, Duan H, Qin Q, et al. Advances in oral drug delivery systems: challenges and opportunities. *Pharmaceutics*. 2023;15(2):484. doi:10.3390/pharmaceutics15020484
12. Selmani A, Seibert E, Tetyczka C, et al. Thiolated chitosan conjugated liposomes for oral delivery of selenium nanoparticles. *Pharmaceutics*. 2022;14(4):803. doi:10.3390/pharmaceutics14040803
13. Song X, Chen Y, Sun H, Liu X, Leng X. Physicochemical stability and functional properties of selenium nanoparticles stabilized by chitosan, carrageenan, and gum Arabic. *Carbohydr Polym*. 2021;255:117379. doi:10.1016/j.carbpol.2020.117379
14. Aljabbari A, Kihara S, Rades T, Boyd BJ. The biomolecular gastrointestinal Corona in oral drug delivery. *J Control Release*. 2023;363:536–549. doi:10.1016/j.jconrel.2023.09.049
15. Nel AE, Mädler L, Velegol D, et al. Understanding biophysicochemical interactions at the nano–bio interface. *Nat Mater*. 2009;8(7):543–557. doi:10.1038/nmat2442
16. Wang C, Chen B, He M, Hu B. Composition of intracellular protein corona around nanoparticles during internalization. *ACS Nano*. 2021;15(2):3108–3122. doi:10.1021/acsnano.0c09649
17. Cui M, Liu R, Deng Z, Ge G, Liu Y, Xie L. Quantitative study of protein coronas on gold nanoparticles with different surface modifications. *Nano Res*. 2014;7(3):345–352. doi:10.1007/s12274-013-0400-0
18. Johnston BD, Kreyling WG, Pfeiffer C, et al. Colloidal stability and surface chemistry are key factors for the composition of the protein corona of inorganic gold nanoparticles. *Adv Funct Mater*. 2017;27(42). doi:10.1002/adfm.201701956
19. Lundqvist M, Augustsson C, Lilja M, et al. The nanoparticle protein Corona formed in human blood or human blood fractions. *PLoS One*. 2017;12(4):e0175871. doi:10.1371/journal.pone.0175871
20. Rodriguez-Quijada C, de Puig H, Sánchez-Purrà M, et al. Protease degradation of protein coronas and its impact on cancer cells and drug payload release. *ACS Appl Mater Interfaces*. 2019;11(16):14588–14596. doi:10.1021/acsami.9b00928
21. Terracciano R, Zhang A, Butler EB, et al. Effects of surface protein adsorption on the distribution and retention of intratumorally administered gold nanoparticles. *Pharmaceutics*. 2021;13(2):216. doi:10.3390/pharmaceutics13020216
22. Ault AP, Stark DI, Axson JL, et al. Protein Corona-induced modification of silver nanoparticle aggregation in simulated gastric fluid. *Environ Sci Nano*. 2016;3(6):1510–1520. doi:10.1039/C6EN00278A
23. Wang Y, Li M, Xu X, Tang W, Xiong L, Sun Q. Formation of protein corona on nanoparticles with digestive enzymes in simulated gastrointestinal fluids. *J Agric Food Chem*. 2019;67(8):2296–2306. doi:10.1021/acs.jafc.8b05702
24. Wang Y, Sun Y, Yang J, et al. Interactions of surface-functionalized starch nanoparticles with pepsin and trypsin in simulated gastrointestinal fluids. *J Agric Food Chem*. 2020;68(37):10174–10183. doi:10.1021/acs.jafc.0c02820
25. Sun Y, Zhen T, Li Y, et al. Interaction of food-grade titanium dioxide nanoparticles with pepsin in simulated gastric fluid. *LWT*. 2020;134:110208. doi:10.1016/j.lwt.2020.110208
26. Wang Y, Zhou L, Sun Y, et al. Formation of protein Corona on interaction of pepsin with chitin nanowhiskers in simulated gastric fluid. *Food Chem*. 2022;383:132393. doi:10.1016/j.foodchem.2022.132393
27. Ullah A, Mu J, Wang F, et al. Biogenic selenium nanoparticles and their anticancer effects pertaining to probiotic bacteria—A review. *Antioxidants*. 2022;11(10):1916. doi:10.3390/antiox11101916
28. Mizrahy S, Peer D. Polysaccharides as building blocks for nanotherapeutics. *Chem Soc Rev*. 2012;41(7):2623–2640. doi:10.1039/C1CS15239D
29. Chen CL, Wang YM, Liu CF, Wang JY. The effect of water-soluble chitosan on macrophage activation and the attenuation of mite allergen-induced airway inflammation. *Biomaterials*. 2008;29(14):2173–2182. doi:10.1016/j.biomaterials.2008.01.023
30. Lee Y, Sugihara K, Gillilland MG, Jon S, Kamada N, Moon JJ. Hyaluronic acid–bilirubin nanomedicine for targeted modulation of dysregulated intestinal barrier, microbiome and immune responses in colitis. *Nat Mater*. 2020;19(1):118–126. doi:10.1038/s41563-019-0462-9
31. Huang TL, Hsu HC, Yao CH, Chen YS, Wang J. Anti-inflammatory and structure protective effects of hyaluronans: are these effects molecular weight dependent? *Biomed Eng*. 2011;23(01):13–20. doi:10.4015/S1016237211002323
32. Guo Z, Cao X, DeLoid GM, et al. Physicochemical and morphological transformations of chitosan nanoparticles across the gastrointestinal tract and cellular toxicity in an in vitro model of the small intestinal epithelium. *J Agric Food Chem*. 2020;68(1):358–368. doi:10.1021/acs.jafc.9b05506
33. Du H, Liu M, Yang X, Zhai G. The design of pH-sensitive chitosan-based formulations for gastrointestinal delivery. *Drug Discov Today*. 2015;20(8):1004–1011. doi:10.1016/j.drudis.2015.03.002
34. Jelkmann M, Menzel C, Baus RA, et al. Chitosan: the one and only? Aminated cellulose as an innovative option for primary amino groups containing polymers. *Biomacromolecules*. 2018;19(10):4059–4067. doi:10.1021/acs.biomac.8b01069
35. Griesser J, Hetényi G, Bernkop-Schnürch A. Thiolated hyaluronic acid as versatile mucoadhesive polymer: from the chemistry behind to product developments—what are the capabilities? *Polymers*. 2018;10(3):243. doi:10.3390/polym10030243

36. Bernkop-Schnürch A. Thiomers: a new generation of mucoadhesive polymers. *Adv Drug Deliv Rev*. 2005;57(11):1569–1582. doi:10.1016/j.addr.2005.07.002
37. Perrone M, Lopalco A, Lopedota A, et al. S-preactivated thiolated glycol chitosan useful to combine mucoadhesion and drug delivery. *Eur J Pharm Biopharm*. 2018;132:103–111. doi:10.1016/j.ejpb.2018.09.015
38. Schmitz T, Hombach J, Bernkop-Schnürch A. Chitosan-N-acetyl cysteine conjugates: *in vitro* evaluation of permeation enhancing and P-glycoprotein inhibiting properties. *Drug Deliv*. 2008;15(4):245–252. doi:10.1080/10717540802006708
39. Griffin S, Sarfraz M, Hartmann S, et al. Resuspendable powders of lyophilized chalcogen particles with activity against microorganisms. *Antioxidants*. 2018;7(2):23. doi:10.3390/antiox7020023
40. Nomanbhoy TK, Cerione RA. Characterization of the Interaction between RhoGDI and Cdc42Hs using fluorescence spectroscopy. *J Biol Chem*. 1996;271(17):10004–10009. doi:10.1074/jbc.271.17.10004
41. Song X, Chen Y, Zhao G, Sun H, Che H, Leng X. Effect of molecular weight of chitosan and its oligosaccharides on antitumor activities of chitosan-selenium nanoparticles. *Carbohydr Polym*. 2020;231:115689. doi:10.1016/j.carbpol.2019.115689
42. Bai K, Hong B, He J, Hong Z, Tan R. Preparation and antioxidant properties of selenium nanoparticles-loaded chitosan microspheres. *Int J Nanomed*. 2017;12:4527–4539. doi:10.2147/IJN.S129958
43. Selmani A, Ulm L, Kasemets K, et al. Stability and toxicity of differently coated selenium nanoparticles under model environmental exposure settings. *Chemosphere*. 2020;250:126265. doi:10.1016/j.chemosphere.2020.126265
44. Bakshi MS. How surfactants control crystal growth of nanomaterials. *Cryst Growth Des*. 2016;16(2):1104–1133. doi:10.1021/acs.cgd.5b01465
45. Budiman A, Nurfadilah N, Muchtaridi M, Sriwidodo S, Aulifa DL, Rusdin A. The impact of water-soluble chitosan on the inhibition of crystal nucleation of alpha-mangostin from supersaturated solutions. *Polymers*. 2022;14(20):4370. doi:10.3390/polym14204370
46. Jog R, Burgess DJ. Pharmaceutical amorphous nanoparticles. *J Pharm Sci*. 2017;106(1):39–65. doi:10.1016/j.xphs.2016.09.014
47. Kumar A, Sevonkaev I, Goia DV. Synthesis of selenium particles with various morphologies. *J Colloid Interface Sci*. 2014;416:119–123. doi:10.1016/j.jcis.2013.10.046
48. Nonsuwan P, Puthong S, Palaga T, Muangsin N. Novel organic/inorganic hybrid flower-like structure of selenium nanoparticles stabilized by pullulan derivatives. *Carbohydr Polym*. 2018;184:9–19. doi:10.1016/j.carbpol.2017.12.029
49. Derakhshan-sefidi M, Bakhshi B, Rasekhi A. Thiolated chitosan nanoparticles encapsulated nisin and selenium: antimicrobial/antibiofilm/anti--attachment/immunomodulatory multi-functional agent. *BMC Microbiol*. 2024;24(1):257. doi:10.1186/s12866-024-03400-7
50. Fröhlich E, Roblegg E. Oral uptake of nanoparticles: human relevance and the role of in vitro systems. *Arch Toxicol*. 2016;90(10):2297–2314. doi:10.1007/s00204-016-1765-0
51. Bonengel S, Bernkop-Schnürch A. Thiomers — from bench to market. *J Control Release*. 2014;195:120–129. doi:10.1016/j.jconrel.2014.06.047
52. Liao YH, Jones SA, Forbes B, Martin GP, Brown MB. Hyaluronan: pharmaceutical characterization and drug delivery. *Drug Deliv*. 2005;12(6):327–342. doi:10.1080/10717540590952555
53. Zhang C, Zhai X, Zhao G, Ren F, Leng X. Synthesis, characterization, and controlled release of selenium nanoparticles stabilized by chitosan of different molecular weights. *Carbohydr Polym*. 2015;134:158–166. doi:10.1016/j.carbpol.2015.07.065
54. Borowska M, Jiménez-Lamana J, Bierla K, Jankowski K, Szpunar J. A green and fast microwave-assisted synthesis of selenium nanoparticles and their characterization under gastrointestinal conditions using mass spectrometry. *Food Chem*. 2023;417:135864. doi:10.1016/j.foodchem.2023.135864
55. Böhmert L, Girod M, Hansen U, et al. Analytically monitored digestion of silver nanoparticles and their toxicity on human intestinal cells. *Nanotoxicology*. 2014;8(6):631–642. doi:10.3109/17435390.2013.815284
56. Peng Q, Liu J, Zhang T, Zhang TX, Zhang CL, Mu H. Digestive enzyme corona formed in the gastrointestinal tract and its impact on epithelial cell uptake of nanoparticles. *Biomacromolecules*. 2019;20(4):1789–1797. doi:10.1021/acs.biomac.9b00175
57. Jeevanantham V, Tamilselvi D, Rathidevi K, Bavaji SR. Greener microwave synthesized Se nanospheres for antioxidant, cell viability, and antibacterial effect. *J Mater Res*. 2023;38(7):1909–1918. doi:10.1557/s43578-023-00965-3
58. Shahabadi N, Zendehcheshm S, Khademi F. Selenium nanoparticles: synthesis, in-vitro cytotoxicity, antioxidant activity and interaction studies with ct-DNA and HSA, HHb and Cyt c serum proteins. *Biotechnol Rep*. 2021;30:e00615. doi:10.1016/j.btre.2021.e00615
59. Zhang P, Zhang N, Wang Q, et al. Disulfide bond reconstruction: a novel approach for grafting of thiolated chitosan onto wool. *Carbohydr Polym*. 2019;203:369–377. doi:10.1016/j.carbpol.2018.09.074
60. Salau VF, Erukainure OL, Ibeji CU, Koorbanally NA, Islam Md S. Ferric-induced pancreatic injury involves exacerbation of cholinergic and proteolytic activities, and dysregulation of metabolic pathways: protective effect of caffeic acid. *Biol Trace Elem Res*. 2020;196(2):517–527. doi:10.1007/s12011-019-01937-7
61. Mateos-Diaz E, Bakala N' Goma JC, Byrne D, Robert S, Carrière F, Gaussier H. IR spectroscopy analysis of pancreatic lipase-related protein 2 interaction with phospholipids: 1. Discriminative recognition of mixed micelles versus liposomes. *Chem Phys Lipids*. 2018;211:52–65. doi:10.1016/j.chemphyslip.2017.02.005
62. Chen Q, Xu S, Liu Q, Masliyah J, Xu Z. QCM-D study of nanoparticle interactions. *Adv Colloid Interface Sci*. 2016;233:94–114. doi:10.1016/j.cis.2015.10.004
63. Shinya S, Fukamizo T. Interaction between chitosan and its related enzymes: a review. *Int J Biol Macromol*. 2017;104:1422–1435. doi:10.1016/j.ijbiomac.2017.02.040
64. Sardar R, Ahmed S, Shah AA, Yasin NA. Selenium nanoparticles reduced cadmium uptake, regulated nutritional homeostasis and antioxidative system in Coriandrum sativum grown in cadmium toxic conditions. *Chemosphere*. 2022;287:132332. doi:10.1016/j.chemosphere.2021.132332
65. Barzegarparay F, Najafzadehvarzi H, Pourbagher R, Parsian H, Ghoreishi SM, Mortazavi-Derazkola S. Green synthesis of novel selenium nanoparticles using Crataegus monogyna extract (SeNPs@CM) and investigation of its toxicity, antioxidant capacity, and anticancer activity against MCF-7 as a breast cancer cell line. *Biomass Convers Biorefin*. 2023;14(20):25369–25378. doi:10.1007/s13399-023-04604-z
66. Chen W, Cheng H, Xia W. Construction of polygonatum sibiricum polysaccharide functionalized selenium nanoparticles for the enhancement of stability and antioxidant activity. *Antioxidants*. 2022;11(2):240. doi:10.3390/antiox11020240
67. Bai K, Hong B, He J, Huang W. Antioxidant capacity and hepatoprotective role of chitosan-stabilized selenium nanoparticles in concanavalin a-induced liver injury in mice. *Nutrients*. 2020;12(3):857. doi:10.3390/nu12030857

68. Xu Q, Zhong T, Li HL. Antioxidant and free radical scavenging activities of N-modified chitosans. *Adv Mat Res*. 2014;1002:91–98. doi:10.4028/www.scientific.net/AMR.1002.91
69. Rushworth GF, Megson IL. Existing and potential therapeutic uses for N-acetylcysteine: the need for conversion to intracellular glutathione for antioxidant benefits. *Pharmacol Ther*. 2014;141(2):150–159. doi:10.1016/j.pharmthera.2013.09.006
70. Mohammed AA, Niamah AK. Identification and antioxidant activity of hyaluronic acid extracted from local isolates of Streptococcus thermophilus. *Mater Today Proc*. 2022;60:1523–1529. doi:10.1016/j.matpr.2021.12.038
71. Theofanous A, Sarli I, Fragou F, Bletsa E, Deligiannakis Y, Louloudi M. Antioxidant hydrogen-atom-transfer to DPPH radicals by hybrids of {Hyaluronic-Acid Components}@SiO_2. *Langmuir*. 2022;38(40):12333–12345. doi:10.1021/acs.langmuir.2c02021
72. Cleland RL, Strauss UP, Helfgott C, et al. Polyelectrolyte properties of sodium hyaluronate. 2. potentiometric titration of hyaluronic acid. *Macromolecules*. 1982;15(2):386–395.
73. Berezney JP, Saleh OA. Electrostatic effects on the conformation and elasticity of hyaluronic acid, a moderately flexible polyelectrolyte. *Macromolecules*. 2017;50(3):1085–1089. doi:10.1021/acs.macromol.6b02166
74. Leichner C, Jelkmann M, Bernkop-Schnürch A. Thiolated polymers: bioinspired polymers utilizing one of the most important bridging structures in nature. *Adv Drug Deliv Rev*. 2019;151-152:191–221. doi:10.1016/j.addr.2019.04.007
75. Ng BC, Chan ST, Lin J, Tolbert SH. Using polymer conformation to control architecture in semiconducting polymer/viral capsid assemblies. *ACS Nano*. 2011;5(10):7730–7738. doi:10.1021/nn202493w
76. Nienhaus K, Nienhaus GU. Mechanistic understanding of protein corona formation around nanoparticles: old puzzles and new insights. *Small*. 2023;19(28). doi:10.1002/smll.202301663
77. Lundqvist M, Stigler J, Cedervall T, et al. The evolution of the protein corona around nanoparticles: a test study. *ACS Nano*. 2011;5(9):7503–7509. doi:10.1021/nn202458g
78. Peng Q, Zhang S, Yang Q, et al. Preformed albumin Corona, a protective coating for nanoparticles based drug delivery system. *Biomaterials*. 2013;34(33):8521–8530. doi:10.1016/j.biomaterials.2013.07.102
79. Pophaly SD, Poonam, Singh P, Kumar H, Tomar SK, Singh R, Singh R. Selenium enrichment of lactic acid bacteria and bifidobacteria: a functional food perspective. *Trends Food Sci Technol*. 2014;39(2):135–145. doi:10.1016/j.tifs.2014.07.006
80. Sadler RA, Mallard BA, Shandilya UK, Hachemi MA, Karrow NA. The immunomodulatory effects of selenium: a journey from the environment to the human immune system. *Nutrients*. 2024;16(19):3324. doi:10.3390/nu16193324
81. Kim KS, Na K, Bae YH. Nanoparticle oral absorption and its clinical translational potential. *J Control Release*. 2023;360:149–162. doi:10.1016/j.jconrel.2023.06.024
82. Wang X, Lei R, Li L, et al. Rearrangement of protein structures on a gold nanoparticle surface is regulated by ligand adsorption modes. *Nanoscale*. 2021;13(48):20425–20436. doi:10.1039/D1NR04813A
83. Kumar S, Parekh SH. Molecular control of interfacial fibronectin structure on graphene oxide steers cell fate. *ACS Appl Mater Interfaces*. 2021;13(2):2346–2359. doi:10.1021/acsami.0c21042